

Report on DELP 1986 Cruises in the Northwestern Pacific

Part 1: General Outline

JAPANESE DELP RESEARCH GROUP ON DEEP STRUCTURE OF OCEANIC LITHOSPHERE

(Received September 27, 1989)

Abstract

In mid-summer of 1986, as part of the Japanese Lithosphere Research Program (DELP: Japanese title of ILP) geophysical DELP research cruises (DELP-86 cruises) were carried out in cooperation with the Earthquake Prediction Research Program of Japan in the northwestern Pacific Basin, between Shatsky Rise and the northern part of the Japanese Islands. The total length of survey lines amounts to about 2100 km along which various observations were made. This report, Parts 1 through 4 of this issue, describes mainly the results of the DELP-86 cruises. Some of the studies on the seismic structure are being continued by the Earthquake Prediction Research Program of Japan. Data and interpretations obtained by others related to the present program are also referred to in the interpretation of the present report (Part 1). Scientists from nine universities and institutions participated in the present study. The scientific objectives, survey area, cruise periods, items of observation, filing of data bases and names of participants in this program are listed in this Part 1. A series of basic data from seismic experiments on the present cruises are presented as a supplement for convenience in further studies. Some results obtained prior to the present survey are also included in the concluding remarks of this part. A configuration of the subducting Pacific Plate underneath Northeast Japan which was traced by using arrivals of sound signal data obtained by the onshore seismic observation network is also mentioned. Further detailed descriptions of individual experiments are given in Parts 2, 3 and 4 of this issue.

1. Scientific Objectives

The scientific objective of DELP-86 is to study the tectonic structure and evolution of the oceanic lithosphere, northwestern Pacific, and its bearing on the tectonic history of the area. It has also a long-range goal to obtain insight into the structure of the deeper part of the oceanic lithosphere and the coupling stiffness between the upper part of the presumably convecting mantle and the bottom of the lithosphere.

2. Introduction

The Pacific Plate is one of the large plates on the globe along with the North American, Eurasian, Philippine, Australian and Antarctic Plates. A large scale lithospheric physiognomy (bathymetric depth, lithosphere thickness and others) of the western part of the Pacific Plate is a normal one similar to that of other large oceanic basins with respect to heat flow vs. age, lithospheric thickness vs. age and bathymetric depth vs. age (YOSHII *et al.*, 1976; DAVIS and LISTER, 1977; PARSONS and SCLATER, 1977; HAYES, 1983). The Pacific Plate is actively colliding with large land masses (*e.g.*, Eurasian or Northamerican Plate) on its western and northwestern edges.

It is claimed through marine geomagnetic studies in the western part of the Pacific that the Pacific Plate evolved from a small basin about 195 Ma ago (in the Jurassic: *e.g.*, HILDE *et al.*, 1977; TAMAKI *et al.*, 1989). Evolution of the Pacific Plate has left a variety of remnant structural relics within and around itself. It is suggested that some of the remnant suture lines observable on the magnetic lineation patterns form a tectonic boundary between fragments within the plate (TAKAGI, 1986). It is also inferred that some of the ancient rifting systems that once acted as spreading centers in the ancient Pacific area had been consumed underneath the North American or Eurasian Plate. The consumption of the Pacific Plate is still occurring along big trench systems: the Kuril-Kamchatka, Japan, Izu-Ogasawara, Mariana, Yap and Palau Trenches.

There have been many studies on structural and tectonic characteristics of the western part of the Pacific area (DEN *et al.*, 1969; YOSHII, 1975; ASADA, 1980; NAGUMO *et al.*, 1981; TOMODA *et al.*, 1982; TOMODA and FUJIMOTO, 1982; ANOSOV *et al.*, 1982; ASADA *et al.*, 1980; CESSARO and DUENNEBIER, 1987; BUTLER and DUENNEBIER, 1987; DUENNEBIER, 1987; SEGAWA and MATSUMOTO, 1987; SHIMAMURA, 1987). The seismic structure of a deeper part of the lithosphere of the western Pacific area is

characterized by variety from place to place (*e.g.*, HOTTA, 1970; JAPANESE DELP RESEARCH GROUP, 1989) and the anisotropic velocity contrast along different azimuthal orientations as revealed by ocean bottom seismic observations (SHIMAMURA *et al.*, 1983) as well as by Rayleigh wave phase velocity (SUETSUGU and NAKANISHI, 1987).

It is also noted that the mechanical coupling between the Pacific Plate and the land masses on its west is much weaker than on its eastern edge based upon occurrence of big earthquakes, *i.e.*, the Mariana Trench in the west compared to the Chile Trench in the east (UYEDA and KANAMORI, 1979). Recent studies on seismic fine structure beneath the landward slope of the central part of the Japan Trench revealed that the stiffness of seismic coupling between the Pacific Plate and the Japanese land mass can be related to the bathymetric features and scars of fault lines in the Pacific Plate east of the Japan Trench (URABE, 1987). It is poorly understood, however, what kind of geometrical as well as mechanical relationships exist between the Pacific and Eurasian (or North American) Plates which have been colliding along the Japan Trench for a long time, at least since the Tertiary.

Back-arc basins on the western to northern corner of the Pacific Plate are believed to be formed as a result of back-arc rifting phenomena. However, some of them show clearly that they could be a remnant of trapped fragments of the Pacific Plate, which was rifted and intruded by subsurface volcanism, sills and dikes, afterward (SHOR and TOKSOZ, 1971; BEN-AVRAHAM *et al.*, 1972; UYEDA and BEN-AVRAHAM, 1972; BEN-AVRAHAM and UYEDA, 1973; COOPER *et al.*, 1976; HILDE *et al.*, 1977; UYEDA and MCCABE, 1983; HILDE and LEE, 1984). In the Japan Sea, there is a significant azimuthal anisotropy in seismic velocity structure and the orientation of higher velocity happens to be parallel to that in the northwestern Pacific as reported by OKADA *et al.* (1978) and HIRATA *et al.* (1989). The disturbance and weak amplitude of marine magnetic lineation patterns of the Japan Sea could be also interpreted as a trapped fragment of the Pacific Plate which was rifted by later multisource volcanic activities (*e.g.*, TAMAKI, 1988). The bathymetric depth of the Japan Sea is quite deep for its age of formation (TAMAKI, ODP data; private comm.) which favors an argument of a part of the Pacific Plate. This point of view, though little accepted by marine geoscientists, has not been ruled out yet even after our recent DELP-85 surveys (*e.g.*, KIMURA *et al.*, 1987).

One of the key factors to understand such a kinematic feature of ocean basin evolution is to obtain the detailed lithospheric internal structure including density profiles, mineralogical profiles, velocity profiles as

well as ductile properties with respect to depths. With these parameters given, we can discuss in turn mechanical and dynamic features of the subducting oceanic lithospheres which induce rifting and opening of back-arc basins. Therefore, the northwestern corner of the Pacific basin is chosen for the present study to meet the requirement of the stated scientific objectives.

DELP-86 cruises comprised two research vessels, Wakashio-maru, Nippon Salvage Company and Dai-3 Kaiko-maru, Tokai Salvage Company. The latter was chartered by courtesy of the Earthquake Prediction Research Program of Japan to do a joint study with the DELP marine research group. Scientists from nine universities and institutions participated in the present study. Further details of the present program are described in following sections.

3. Cruise period

Cruise DELP-86 WAKASHIO (Wakashio-maru) and KAIKO (Dai-3 Kaiko-maru)

***WAKASHIO

July 10, 1986 Departure from Chuo, Chiba.

14-18, Deployment of OBS's (Ocean Bottom Seismometer).

19-24, Explosion of small dynamite charges and a large volume Airgun shooting.

25-27, Explosion of big dynamite charges.

28-31, Recovery of OBS's.

Aug. 1, Heat Flow experiment.

3, Back to Chiba.

July 10-Aug. 3, Magnetic measurement all along steaming tracks.

***KAIKO

July 13, 1986 Departure from Nittsu, Muroran, Hokkaido.

14-18, Deployment of OBS's.

19-24, Explosions of large dynamite charges.

25-28, Recovery of OBS's.

31, Back to Muroran.

July 13-31 Magnetic measurement all along steaming tracks.

4. Items of observation

- 1) 12 KHz precision Depth Recording.
- 2) 3.5 KHz Depth Recording.
- 3) Single-channel Seismic Profiling.

- 4) Ocean Bottom Seismometer Experiment (30 stations).
 - 4)-1 Structure.
 - 4)-2 Seismicity.
- 5) Geomagnetic Survey.
 - 5)-1 Total force.
 - 5)-2 Three-axis vector component.
- 6) Heat Flow Survey.

5. Data filing and processing

- 1) Track positioning.
- 2) Depth record (digitized) for whole track lines.
- 3) Shot times of large volume Airgun.
- 4) Shot times of explosions.
- 5) Geomagnetic elements (H_x , H_y , H_z and F).
- 6) Seismic wave form (digitized).

6. Participants

Earthquake Research Institute, University of Tokyo

S. NAGUMO, T. KORESAWA, and H. KATAO.

Laboratory for Ocean Bottom Seismology, Hokkaido University

H. SHIMAMURA, and T. IWASAKI.

Observation Center for Prediction of Earthquakes and Volcanic Eruptions,
Tohoku University

A. NISHIZAWA, and S. NAKAO.

Institute of Geophysics, University of Tokyo

T. KANAZAWA, N. HIRATA (now, Chiba Univ.), and N. TOMITA.

Department of Earth Sciences, Chiba University

H. KINOSHITA (now, Earthquake Res. Inst., Univ. Tokyo), K. SUYEHRO
(now, Ocean Res. Inst., Univ. Tokyo), T. IIDAKA (now, Earthquake Res.
Inst., Univ. Tokyo), Y. KAIHO (now, Geophysical Inst., Univ. Tokyo),
M. SUEMASA (now, D. G. Co.), K. YAMAKI (now, Hot Sp. Inst. Kana-
gawa Pref.), N. MATSUDA (now, NEC), R. MORIJIRI (now, Geol. Surv.
Japan), S. ABE, T. IIMURA (now, Fujitsu Comp. Eng. Co.), Y. KASUMI
(now, Yokogawa Denki Co.), N. KOCHI (now, NEC Eng.), T. FUJII
(now, FACOM HITAC Co.), and Y. NAKASA

Department of Oceanography, Tokai University

H. BABA.

Department of Earth Sciences, Kobe Univ.

N. ISEZAKI, T. OUCHI, I. UNO (now, Ocean Res. Inst., Univ. Tokyo),
C. ITOTA, M. KONISHI (now, Daiwa Bank), and M. NAKANISHI (now,
Ocean Res. Inst., Univ. Tokyo).

Department of Physics, Kyushu University

T. URABE (now, Earthquake Res. Inst., Univ. Tokyo).

7. Main operations

The area surveyed by the DELP-86 cruises is shown in Fig. 1. Detailed track lines of the present cruises are given Fig. 2. Geophysical surveys of DELP-86 cruises are mostly concentrated on seismic studies of the lithospheric and crustal structures and geomagnetic measurements of the area. Seismic surveys were performed by combination of ocean bottom seismometers (OBS or OBSH: a hydrophone attached to OBS) and explosives and airgun shootings. Sound signals of big explosions were detected also at onshore seismic observatories in Northeast Japan. Natural earthquakes occurred during the cruise period will be also analysed using the seismic records of OBS deployed for structural studies. Geomagnetic surveys were run by use of both a three-axis magnetometer and a proton precession magnetometer. Underway geomagnetic and topographic surveys were carried out on the steaming tracks from port to survey area and back. Heat flow measurements were only successful on one run during the cruise period. Some parameters obtained in these operations are described below. The main results of these operations will be described in this report and in the individual parts (Part 2, 3 and 4) of this issue in detail.

7-1 Ocean Bottom Seismometer

Thirty sets of OBS were deployed along two track lines, of which 7 sets are offered from the Earthquake Research Institute, 20 from Hokkaido University, and Geophysical Institute, University of Tokyo, and Tohoku University and 3 from Chiba University. Position and water depths of the OBS stations are listed in Table 1. The total length of the survey track lines amounts to about 2,100 km, of which the NNW-SSE branch extends 700 km, and the WSW-ENE line extends about 1400 km, respectively. Big and small charge explosives and large volume (36 liter) airgun array shootings were run along these track lines. Unfortunately, a new compressor system went down half way through the operation. After the accident we had to use a number of small charge explosives instead of the airgun. Positions and water depths of the big explosion stations are

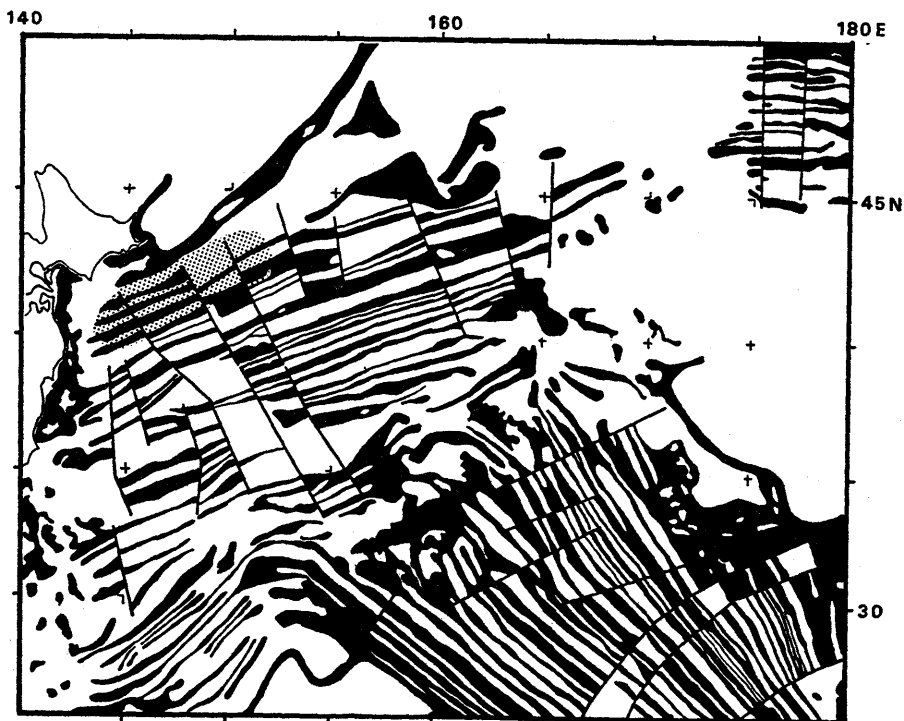


Fig. 1. Sketch map of survey area (shaded) run by DELP-86 program with magnetic anomaly stripes in the northwestern Pacific. Black stripes show negative geomagnetic anomaly. Copy made from ISEZAKI (1987).

listed in Table 2. Shot numbers for larger weight dynamite charges are given by two digits (from 01 to 22) right after "SHOT" (sometimes omitted in some figures of appendix A) and those for smaller charges are given by three digits (starting from 201) for convenience of sorting. Distribution of the OBS stations is shown in Fig. 2. Positions of the big explosions as well as airgun shootings plus small charge explosions are shown in Fig. 3.

We have tried a line of condensed explosive shootings along a small fraction of the track line (HDS) in the NNW-SSE branch as indicated in Fig. 3. The position and other parameters for this portion are listed in Table 3. A blow up of the high density shooting positions is shown in Fig. 4. Original record sections (series of figures in appendix A) of arrival time versus distance which are pasted up on a single sheet for individual OBS's are presented in the appendix of this part. A preliminary result of analysis on the seismic structure of upper part of the lithosphere of a fraction of the surveyed area is shown in Fig. 5 (refer also to SEKIHARA,

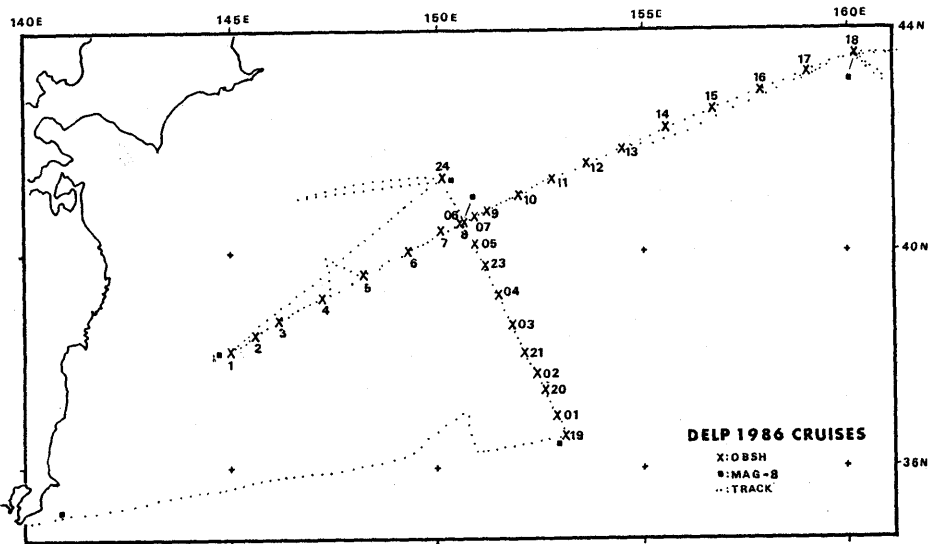


Fig. 2. Survey lines (dotted lines) and stations of cruises DELP-86, WAKASHIO and KAIKO, for the study on the deep structure of oceanic lithospheric plate in the northwestern Pacific Basin. Symbols denote: MAG-8, Calibration of 3-axis and total force of Magnetometer Systems. OBS (crosses), Stations for Ocean Bottom Seismographs. Geographic position of OBS stations are listed in Table 1.

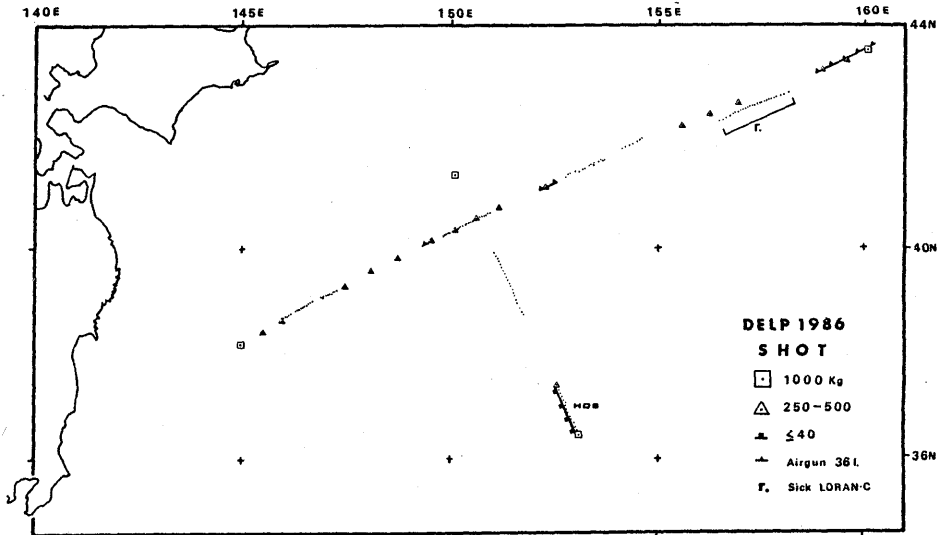


Table 1. Geographic coordinates and water depths of the position OBS stations. EOBS's are operated by Earthquake Research Institute, University of Tokyo and TOBS's were supplied by Geophysical Institute, University of Tokyo and the rest of participants in the present cruises. Dates of deployment are all in July. Day, hour and minute are marked by full stops. Latitude and longitude are given in degrees, minutes and seconds with full stops among them. Bathymetric water depth is given in meters.

*1: Numbering used in operations. *2: Numbering used in analyses.

No. 1 *1	No. 2 *2	Date of deployment	Latitude (deg. N)	Longitude (deg. E)	Water Depth (meters)
P1	TOBS01		38. 11. 86	145. 00. 15	5296
P2	TOBS02		38. 28. 23	145. 35. 89	5320
P3	TOBS03		38. 44. 20	146. 11. 66	5284
P4	TOBS04		39. 09. 81	146. 12. 36	5402
P5	TOBS05		39. 35. 75	148. 14. 41	5473
P6	TOBS06		40. 00. 46	149. 17. 47	5330
P7	TOBS07		40. 20. 38	150. 06. 60	5405
P8	TOBS08		40. 32. 48	150. 38. 16	5427
P9	TOBS09	16. 02. 23	40. 45. 61	151. 13. 00	5502. 6
P10	TOBS10	16. 07. 32	41. 01. 91	151. 58. 40	5301. 7
P11	TOBS11	16. 13. 27	41. 19. 31	152. 47. 16	5902. 4
P12	TOBS12	16. 17. 37	41. 36. 33	153. 36. 32	5545. 6
P13	TOBS13	16. 21. 33	41. 52. 73	154. 25. 52	5476. 0
P14	TOBS14	17. 02. 55	42. 14. 32	155. 32. 13	5596. 8
P15	TOBS15	17. 08. 10	42. 35. 06	156. 39. 16	5452. 0
P16	TOBS16	17. 13. 22	42. 55. 46	157. 47. 59	5561. 4
P17	TOBS17	17. 16. 30	43. 15. 32	158. 57. 03	5563. 9
P18	TOBS18	17. 23. 37	43. 33. 40	160. 05. 75	5349. 0
P19	TOBS19	14. 07. 12	36. 29. 12	153. 07. 68	5698. 3
P20	TOBS20	14. 16. 38	37. 23. 83	152. 35. 49	5920. 1
P21	TOBS21	15. 00. 08	38. 06. 76	152. 09. 96	5861. 2
P22	No OBS	deployed.			
P23	TOBS23	15. 14. 55	39. 44. 08	151. 09. 76	5391. 6
P24	TOBS24		41. 20. 50	150. 06. 60	5250
E1	EOBS1	14. 11. 29	36. 53. 56	152. 52. 86	5644. 0
E2	EOBS2	14. 19. 53	37. 42. 28	152. 24. 47	5771. 0
E3	EOBS3	15. 05. 30	38. 39. 15	151. 49. 77	5685. 0
E4	EOBS4	15. 10. 17	39. 11. 67	151. 29. 72	5472. 0
E5	EOBS5	15. 18. 11	40. 08. 28	150. 54. 18	5389. 0
E6	EOBS6	15. 21. 40	40. 32. 51	150. 38. 35	5431. 8
E7	EOBS7	15. 23. 52	40. 38. 74	150. 55. 73	5401. 1

1990; SEKIHARA and MARINE LONG SHOT RESEARCH GROUP OF JAPAN 1990). The fine configuration may be refined after more detailed analysis in the future.

Fig. 3. Positions of explosive and large volume airgun shootings. Volume of the airgun chamber is 36 liters. Sick LORAN-C denotes that the allocation of the ships position by use of LORAN-C system malfunctioned and dead reckoning measure was taken for this interval. High density shooting with small dynamite charges was done on section HDS along the NNW-SSW branch of the track line. Weights of explosives are given by various symbol marks with numbers (kg) in the legend. Dotted lines are portions of airgun shootings.

Table 2. Shot times and geographic positions of large weight explosions. Explosions with charges heavier than 250 kg are shown except for SHOT02-1. Numbers and units are the same as for Table 1.

Shot No.	Weight (Kg)	Time	Latitude (deg. N)	Longitude (deg. E)	Water Depth (meters)
SHOT01	1,000	24.07.20	38.11.02	145.00.16	W. end
SHOT02-1	25	19.18.40	38.25.40	145.29.32	5311.7
SHOT02-2	500	19.18.40	38.25.35	145.30.15	5316.3
SHOT03	500	20.05.39	38.38.82	146.00.25	5270.1
SHOT04 (NG)	250	20.17.34	39.16.44	147.31.48	5345.0
SHOT05	500	21.05.01	39.33.26	148.08.45	5446.0
SHOT06	500	21.09.00	39.48.23	148.45.91	5504.7
SHOT07	500	21.14.36	40.07.99	149.35.69	3740.0
SHOT08	500	21.18.32	40.20.26	150.06.75	(P07) 5441.0
SHOT09	300	21.22.04	40.32.44	150.38.73	(P08) 5435.0
SHOT10	500	22.05.04	40.44.36	151.10.83	(P09) 5442.2
SHOT11	500	22.11.27	41.07.77	152.15.19	5301.8
SHOT12	300	22.15.30	41.21.42	152.54.19	5155.2
SHOT13	500	21.19.31	41.34.98	153.33.35	5568.7
SHOT14	500	23.06.30	42.14.28	155.32.71	5593.1
SHOT15	500	23.10.30	42.26.89	156.13.00	5039.8
SHOT16	500	23.14.30	42.39.22	156.53.61	5414.0
SHOT17	500	24.10.20	43.14.18	158.57.02	(P17) 5560.4
SHOT18	500	24.13.23	43.24.52	159.32.02	5410.0
SHOT19	1,000	19.12.52	43.34.23	160.04.45	E. end 5360.0
SHOT20	1,000	27.16.15	36 28.56	153.07.76	S. end 5704.8
SHOT21	500	27.06.05	37. 4.30	152.35.94	(P20) 5883.9
SHOT22	1,000	25.13.17	41.20.56	150.05.36	N. end 5237.7

(P_{xx}) denotes that the shot point is right on top of the OBS position. NG is an unsuccessful shot. E, W, S and N end are end points along track lines. Dates are all in July, 1986.

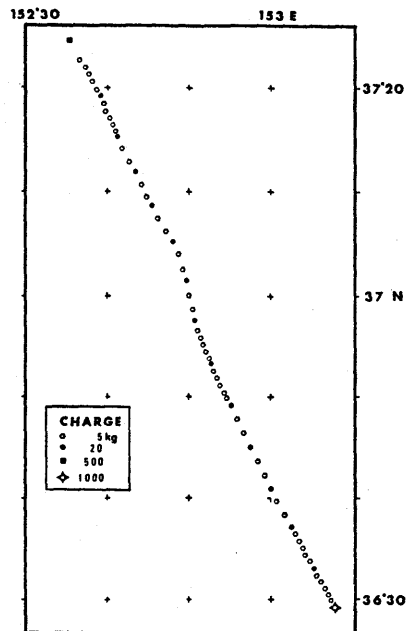


Fig. 4. Blow up distribution of large and small explosions along a survey line of the high density shooting (HDS in Fig. 3) experiment.

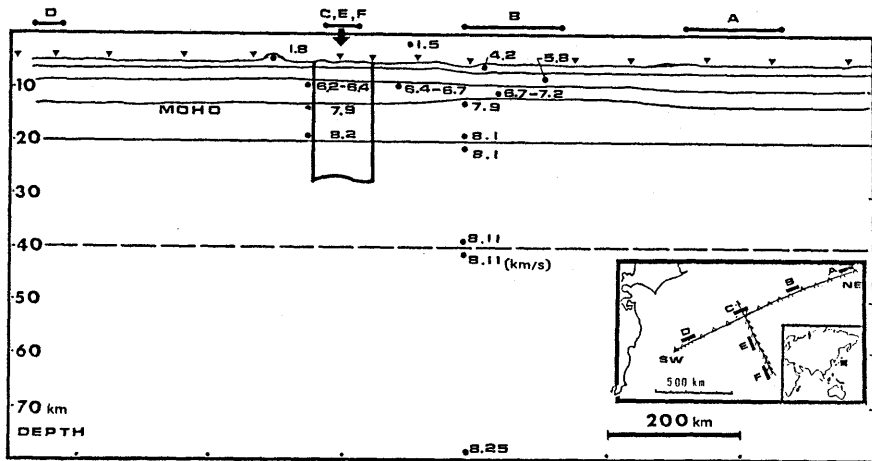


Fig. 5. Preliminary result of analyses on the seismic cross section of the deeper part of lithospheric plate along WSW-ENE track line (1400 km between OBS stations SW and NE in the inset) in the northwestern Pacific Basin. Some results from NNW-SSE track line are synthesized as shown in a thick box frame below a thick arrow. Thick bars numbered by A through F are showing portions of concentrated seismic shooting. Dotted line at the depth of 40 km is assumed tentatively as a boundary between different velocity gradient for best fit in interpreting distant phases in the seismic record sections. This figure is obtained by modifying a figure in the report by SEKIHARA (1990).

7-2 Onshore Observation of Sound Waves from Explosions

Some large weight dynamite explosions detonated along WSW-ENE and NNW-SSE track lines were caught by the seismic network of Tohoku University (Fig. 6, HASEGAWA *et al.*, 1988). In spite of the small amount of explosives, the arrivals at epicentral distances up to 800 km could be well observed due to low seismicity around shot stations. A model of seismic structure across the Japan Trench is constructed by incorporating the crust and upper mantle structures given by many investigations to date (*e.g.*, YOSHII and ASANO, 1972) by the 2-dimensional ray tracing method (CERVENY and PSENCIK, 1981). The positions of the wavespeed boundaries in the model were corrected for the spherical earth. It is assumed that the oceanic lithosphere (Pacific Plate) consists of three distinctive layers. The present data can be used for an experimental check of the large scale structure of the lithospheric plate subducting underneath the Japanese main island. The features of subducting Pacific lithosphere and the lower part of the crust beneath the Northeast of Japan implied through present experiments is presented in Fig. 7. More detailed descriptions on the analyses and assumptions introduced are given by NAKAO *et al.* (1988).

Table 3. Shot times and positions of dynamite charges for the high density shooting experiment. Numbers and units are the same as for Tables 1 and 2. Shots were all on July 27th: hour and minute are divided by full stops and occasionally down to second figures are added. Degree of latitude and longitude are partly omitted when they are equal to those in the upper data line.

Shot No.	Weight (Kg)	Time (1986. 07. 27)	Latitude (deg N)	Longitude (deg E)	Water Depth (meter)
21	500	05. 47	37. 24. 62	152. 35. 27	5875. 6
227	5	07. 46	22. 79	36. 56	5867
228	5	07. 52	22. 10	37. 26	
229	5	07. 58	21. 37	37. 70	
230	5	08. 04	20. 64	38. 22	
231	5	08. 10	19. 95	38. 73	
232	20	08. 15. 30	19. 18	39. 08	
233	5	08. 21	18. 48	39. 53	
234	5	08. 26	17. 75	39. 74	
235	5	08. 32	17. 11	40. 22	
236	5	08. 37	16. 46	40. 67	
237	5	08. 43	15. 74	40. 97	
238	20	08. 47	15. 33	41. 21	
239	5	09. 00	14. 10	41. 79	
240	5	09. 11	12. 80	42. 75	
241	20	09. 20	11. 85	43. 39	5754
242	5	09. 33	10. 63	44. 13	5820
243	5	09. 44	09. 61	44. 76	
244	20	09. 52	08. 69	45. 38	5781
245	5	10. 06	07. 49	46. 23	
246	5	10. 17	06. 21	47. 14	
247	20	10. 25	05. 27	47. 96	
248	5	10. 39	04. 05	48. 73	
249	5	10. 50	02. 60	49. 20	
250	20	10. 59	01. 53	49. 64	5775
251	5	11. 12	00. 02	50. 03	
252	5	11. 23	36. 58. 54	50. 51	
253	20	11. 31	57. 41	50. 77	
254	5	11. 40. 30	56. 57	51. 08	
255	5	11. 46	55. 85	51. 41	
256	5	11. 51	55. 18	51. 77	
257	5	11. 57	54. 44	52. 05	
258	5	12. 02. 30	53. 75	52. 43	
259	20	12. 06	53. 30	52. 68	
260	5	12. 16	52. 54	53. 02	
261	5	12. 21. 30	51. 84	53. 41	
262	5	12. 27	51. 15	53. 87	
263	5	12. 32. 30	50. 44	54. 28	
264	5	12. 38	49. 78	54. 71	
265	20	12. 43	49. 04	55. 05	
266	5	12. 55	47. 63	55. 92	
267	5	13. 06	46. 28	56. 69	
268	20	13. 17	44. 92	57. 46	
269	5	13. 28	43. 61	58. 38	
270	5	13. 39	42. 21	59. 17	
271	20	13. 50	40. 94	153. 00. 01	
272	5	14. 01	39. 58	00. 77	
273	5	14. 12	38. 26	01. 65	
274	20	14. 23	36. 95	02. 50	
275	5	14. 28. 30	36. 34	02. 96	
276	5	14. 34	35. 67	03. 35	
277	5	14. 39. 30	35. 05	03. 79	
278	5	14. 45	34. 38	04. 19	
279	5	14. 50	33. 75	04. 67	
280	20	14. 56	33. 08	05. 12	
281	5	15. 01. 30	32. 40	05. 52	
282	5	15. 07	31. 73	05. 98	
283	5	15. 12. 30	31. 09	06. 44	
284	5	15. 18	30. 41	06. 85	
285	5	15. 23. 30	29. 73	07. 18	
20	1,000	15. 57	29. 07	07. 66	

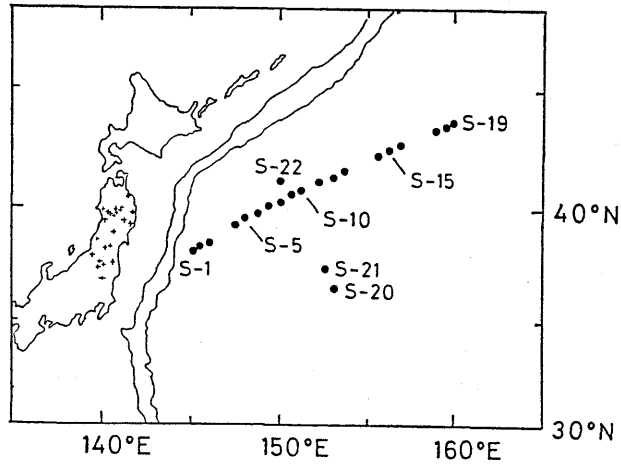


Fig. 6. Locations of shot points (solid circles) and microearthquake observation stations of Tohoku University (crosses). Charge size of S19, S20 and S22 is 1 ton and the others are 300 or 500 kg.

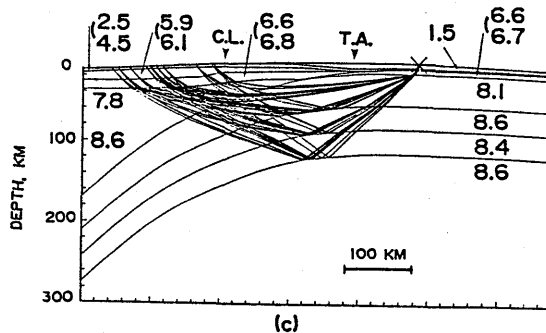


Fig. 7. Cross section of upper mantle and subducting Pacific lithosphere underneath northeast of Honshu, Japan (NAKAO *et al.*, 1988). TA: Japan Trench axis. CL: Coast line of NE Japan.

7-3 Natural Seismicity caught by the OBS

Small and large natural earthquakes of magnitude larger than 3.8 (determination by Japan Meteorological Agency) were detected by a number of OBS's during the present operations. Dates, locations and depths of these earthquakes are listed in Table 4. Epicenters of these earthquakes are plotted in Fig. 8. The earthquakes will be analyzed at the Earthquake Research Institute, University of Tokyo and report will be presented separately.

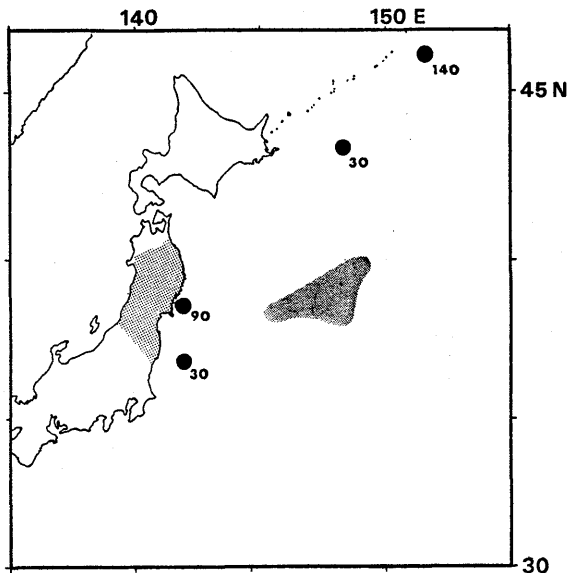


Fig. 8. Distribution of epicenters of natural earthquakes observed by the OBS during the DELP-86 cruises. Detailed positions are listed in Table 4. Shaded areas show the present survey area on the sea and distribution of onshore seismic observatories. Solid numbers indicate depths of earthquake foci in km.

Table 4. Locations and times of occurrence of natural earthquakes observed by OBS's during the present cruises. Time is given in day, hour, minute, second and deci-second, each divided by full stops. Positions are given in degrees, minutes and seconds.

No.	Ms *1	Time (July, 1986)	Latitude (deg N)	Longitude (deg E)	Depth (Km)
1.	6.4	19. 14. 59. 41. 0	46. 05. 50	151. 38. 60	142
2.	4.4	22. 15. 12. 28. 2	38. 32. 80	141. 52. 60	89
3.	4.4	25. 08. 24. 10. 0	43. 21. 60	147. 36. 60	31
4.	3.8	25. 23. 58. 15. 4	36. 55. 70	141. 49. 00.	33

*1: Magnitude determined by Japan Meteorological Agency.

7-4 Geomagnetic Surveys

The three-component magnetometer on board the research vessel and a proton precession magnetometer were run through the entire period of DELP-86 cruises. On board magnetometer system has to be calibrated when the ship changed its latitudinal positions considerably. This measure is achieved on an assumption that there is a significant change in magnetic field along latitude lines. The change in the inclination of the geomagnetic field influences the magnetization of steel vessels, remanent as well as

induction. The calibration was done by turning the vessels bearing around by 360 degrees twice in opposite senses.

8. Main Results

Collection of data available to date prior to this experiment indicates that the oceanic basin of the northwestern Pacific is characterized by the following features.

1. The basin is clearly marked with magnetic stripes of Cretaceous to Jurassic ages with a conspicuous magnetic byte in the vicinity of Shatsky Rise (ISEZAKI, 1987; Fig. 1 of this report).

2. The seismic velocity structure seems to be anisotropic and the axis of higher velocity strikes NNW-SSE with velocity difference about 5-7% (SHIMAMURA *et al.*, 1983).

3. There are several fracture zones running NNW-SSE, nearly parallel to the higher velocity axis of seismic structure. The fracture patterns can be traced on magnetic lineation charts all over the northwestern corner of the Pacific Basin (review by ISEZAKI, 1987).

4. Seismic structure of the Shatsky Rise shows a character similar to the continental cross section (DEN *et al.*, 1969).

5. There must be some tectonic events around 123 Ma (M-3) which induced a drastic change in trends of magnetic lineation patterns in this area, near Shatsky Rise. The cause and duration of the episode, however, could not be determined yet (review by ISEZAKI, 1987).

The scientific results obtained through DELP-86 cruises are as follows.

1. Seismic refraction study revealed that there is a steep wave speed gradient in the upper part of the oceanic basement. The wave speed in this portion seems to be smaller than that accepted for normal oceanic basins (Part 2, this issue).

2. The Moho boundary could be constrained at water depth 8-9 km, which is in general agreement with those obtained by the USSR (ANOSOV, 1982) and DSDP (DUENNEBIER, 1987) experiments (Part 3, this issue; SEKIHARA, *et al.*, 1990).

3. There is possibly a sub-moho boundary in velocity structure with small gradient. This feature is observed in general from place to place in the surveyed area (Part 3, this issue; SEKIHARA, 1990).

4. The oceanic basement, *i.e.*, source of magnetic lineation patterns, is fragmented along a number of fault lines. Magnetic lineation patterns change considerably beyond fracture lines (Part 4, this issue).

5. A large scale horizontal anisotropy in seismic Pn wave velocity of

the lithosphere seems to be small with higher values in NNW-SSE direction. The apparent velocity contrast along different azimuthal orientations may be explained also by a large lateral heterogeneity. This problem has to be contemplated by further analyses on seismic records obtained by this program (Parts 2 and 3, this issue; SEKIHARA, 1990).

Acknowledgments

Participants in this program are grateful to crews on board research vessels who dedicated themselves to running the present program through the entire cruise period. The research is supported by Government grants-in-aid to the universities for geoscience research by the Ministry of Education, Science and Culture, Japan.

References

- ANOSOV, G., V. ARGENTOV and H. GNIBIDENKO, 1982, Crustal low velocity zone south of Shatsky Rise, northwest Pacific ocean, *Geomarine Lettr.*, 2, 17-21.
- ASADA, T., 1980, Studies on the upper mantle structure and anisotropy in the north-western Pacific (in Japanese), *Res. Note of Sci. Fund, Japan*, cont. No. 342014.
- ASADA, T., H. SHIMAMURA and S. ASANO, 1980, Explosion seismological experiments on long-range profiles in the northwestern Pacific and the Mariana seas, *Geodynamics Ser.*, edit. T. W. C. HILDE.
- BEN-AVRAHAM, Z., Z. C. BOWIN and J. SEGAWA, 1972, An extinct spreading center in the Philippine Sea, *Nature*, 240, 453-455.
- BEN-AVRAHAM, Z. and S. UYEDA, 1973, The evolution of the China Basin and the Mesozoic paleogeography of Borneo, Earth Planet, *Sci. Lettr.*, 13, 365-376.
- BUTLER, R. and F. K. DUENNEBIER, 1987, Teleseismic observation from OSS IV, Init. Rept. DSDP, Leg 88, 147-154.
- CERVENY, V. and I. PSENCIK, 1981, SEISS1, A 2-D Seismic Ray Package, Charles University, Prague.
- CESSARO, R. K. and F. K. DUENNEBIER, 1987, Regional earthquakes recorded by ocean bottom seismometers (OBS) and an ocean sub-bottom seismometer (OSS IV) on Leg 88, Init. Rept. DSDP, Leg 88, 129-146.
- COOPER, A. K., M. S. MARLOW and D. W. SCHOLL, 1976, Mesozoic magnetic lineations in the Bering Sea marginal basin, *J. Geophys. Res.*, 8, 1916-1934.
- DAVIS, E. E. and C. R. B. LISTER, 1977, Heat flow measured over the Juan de Fuca Ridge: Evidence for widespread hydrothermal circulation in a highly transportive crust, *J. Geophys. Res.*, 82, 4845-4860.
- DEN, N., W. J. LUDWIG, S. MURAUCHI, J. I. EWING, H. HOTTA, N. T. EDGAR, T. YOSHII, T. ASANUMA, K. HAGIWARA, T. SATO and S. ANDO, 1969, Seismic-refraction measurements in the northwest Pacific basin, *J. Geophys. Res.*, 74, 1421-1434.
- DUENNEBIER, F. K., 1987, The 26 May 1983 Japan Sea Earthquake recorded by OSS IV, Init. Rept. DSDP, Leg 88, 155-160.
- HASEGAWA, A., T. UMINO, A. YAMAMOTO and A. TAKAGI, 1988, Explosions in the North-western Pacific Ocean detected by automatic event detection and location system (in

- Japanese with English abstract), *Zisin*, 41, 609-615.
- HAYES, D. E., 1983, Global studies of ocean crustal depth-age relationships, *EOS Trans, AGU*, 64, 760.
- HILDE, T. W. C., S. UYEDA and L. KROENKE, 1977, Evolution of the western Pacific and its margin, *Tectonophys.*, 38, 145-165.
- HILDE, T. W. C. and C. S. LEE, 1984, Origin and evolution of the west Philippine Basin: A new interpretation, *Tectonophys.*, 102, 85-104.
- HIRATA, N., H. TOKUYAMA and T. W. CHUNG, 1989, An anomalously thick layering of the crust of the Yamato Basin, southeastern Japan Sea: ceasing stage of a back-arc spreading, *Tectonophys.*, 165, 303-314.
- HOTTA, H., 1970, A crustal section across the Izu-Ogasawara arc and trench, *J. Phys. Earth*, 18, 125-141.
- ISEZAKI, N., 1987, Shatsky Rise and marine magnetic anomaly patterns (in Japanese), *Mar. Sci. Month.*, 19, 348-353.
- JAPANESE DELP RESEARCH GROUP ON BACK-ARC BASINS, 1989, Report on DELP Cruise in the Ogasawara Area, Part 1 through 7, *Bull. Earthq. Res. Inst. Univ. Tokyo*, 64, 119-254.
- KIMURA, M., T. MATSUDA, H. SATO, I. KANEOKA, H. TOKUYAMA, S. KURAMOTO, A. OSHIDA, K. SHIMAMURA, K. TAMAKI, H. KINOSHITA and S. UYEDA, 1987, Report on DELP 1985 cruises in the Japan Sea, Part VII—Topography and geology of the Yamato Basin and its vicinity, *Bull. Earthq. Res. Inst., Univ. Tokyo*, 62, 433-446.
- NAGUMO, S., T. OUCHI, J. KASAHARA, S. KORESAWA, Y. TOMODA, K. KOBAYASHI, M. ODEGARD and G. SUTTON, 1981, Sub-moho seismic profiles in the Mariana basin by OBS long range explosion, *Earth Planet. Sci. Lettr.*, 53, 93-102.
- NAKAO, S., A. NISHIZAWA, A. TAKAGI, T. IDAKA, K. SUYEHIRO, H. KINOSHITA and H. SHIMAMURA, 1988, Land observation of the big explosions detonated in the northwestern Pacific Ocean (in Japanese with English abstract), *Zisin*, 41, 125-129.
- OKADA, H., T. MORIYA, T. MATSUDA, T. HASEGAWA, S. ASANO, K. KASAHARA, A. IKAMI, H. AOKI, Y. SASAKI, N. HARUKAWA and K. MATSUMURA, 1978, Velocity anisotropy in the Sea of Japan as revealed by big explosions, *J. Phys. Earth*, 26S, 491-502.
- PARSONS, B. and J. G. SCLATER, 1977, An analysis of the variation of ocean floor bathymetry and heat flow with age, *J. Geophys. Res.*, 82, 803-827.
- SEKIHARA, Y., 1990, Velocity structure of oceanic lithosphere in the northwestern Pacific Basin determined from long shot experiment, Thesis for Deg. M. S., Hokkaido University.
- SEKIHARA, Y. and MARINE LONG SHOT RESEARCH GROUP OF JAPAN, 1990, Seismic deep structure of Pacific Plate in the northwestern Pacific Basin, Abst. No. A12-07, Spring Meet., Seis. Soc. Japan.
- SEGAWA, J. and T. MATSUMOTO, 1987, Free air gravity anomaly of the world ocean as derived from satellite altimeter data, *Bull. Ocean Res. Inst., Univ. Tokyo*, 25 (full volume of a special issue).
- SHIMAMURA, H., T. ASADA, K. SUYEHIRO, T. YAMADA and H. INATANI, 1983, Long shot experiments to study velocity anisotropy in the oceanic lithosphere of the northwestern Pacific, *Phys. Earth Planet. Inter.*, 31, 348-362.
- SHIMAMURA, H., 1987, Ocean bottom seismographic observations in the earthquake prediction project in Japan, Symp. on Earthquake Prediction, 143-151.
- SHOR, N. and M. N. TOKSOZ, 1971, 1971, Evolution of marginal basin, *Nature*, 233, 548-550.
- SUETSUGU, D. and I. NAKANISHI, 1987, Regional and azimuthal dependence of phase velocities of mantle Rayleigh waves in the Pacific Ocean, *Phys. Earth Planet. Int.*, 47, 230-245.

- TAKAGI, A., 1986, Seismotectonics in Japan Trench, Northeast of Japan and back-arc systems (in Japanese), *Earth Month.*, 85, 402-415.
- TAMAKI, K., 1988, Geological structure of the Japan Sea and its tectonic implications, *Bull. Geol. Surv. Japan*, 39, 269-365.
- TAMAKI, K., M. NAKANISHI, K. SAYANAGI and K. KOBAYASHI, 1989, Identification of Jurassic magnetic stripes in the Mariana Basin, Abst. No. B-96, Fall Meet., Seis. Soc. Japan.
- TOMODA, Y. and H. FUJIMOTO, 1982, Maps of gravity anomalies and bottom topography in the western Pacific and reference book for gravity and bathymetric data, *Bull. Ocean Res. Inst., Univ. Tokyo*, 14, (special issue).
- TOMODA, Y., H. FUJIMOTO, T. MATSUMOTO and Y. KONO, 1982, Residual gravity anomalies of the Hawaiian Seamounts and anomalies of the thickness of lithosphere (in Japanese with English abstract), *Zisin*, 35, 291-301.
- URABE, T., 1987, Seismological Regionality of the Middle Japan Trench (Fukushima-Oki) revealed by Ocean Bottom Seismography, PhD Thesis, Univ. Tokyo.
- BEN-UYEDA, S. and Z. AVRAHAM, 1972, Origin and development of the Philippine Sea, *Nature Phys. Sci.*, 240, 176-178.
- UYEDA, S. and H. KANAMORI, 1979, Back-arc opening and the subduction, *J. Geophys. Res.*, 84, 1049-1061.
- UYEDA, S. and R. MCCABE, 1983, A possible mechanism of episodic spreading of the Philippine Sea, in "Accretion Tectonics in the Circum-Pacific Regions, edit. HASHIMOTO, M. and UYEDA", Terra Sci. Pub. Co., 291-306.
- YOSHII, T. and S. ASANO, 1972, Time-Term Analysis of Explosion Seismic Data, *J. Phys. Earth*, 20, 47-57.
- YOSHII, T., 1975, Regionality of group velocities of Rayleigh waves in the Pacific and thickening of the plate, *Earth Planet. Sci. Lettr.*, 25, 305-312.
- YOSHII, T., Y. KONO and K. ITO, 1976, Thickening of the oceanic lithosphere, in "The geophysics of the Pacific Ocean Basin and Its Margins, edit. SUTTON, G.H. et al.", *Geophys. Monogr. Ser., AGU*, 19, 423-430.

Appendix

Record Sections of Explosion Sound Waves.

Sound signals recorded by OBS's (or OBSH's) were digitized and reformed by use of computerized data processing systems. The epicentral distances between OBS and the sound sources were calculated by using arrival times of the water break combined with the water depths of the OBS. After these editing procedures, the time-distance sections of the filtered wave records are displayed on a high speed laser printer connected to computer systems.

Examples of waves after band-pass filtering are shown in Figs. A1 through A3. They were processed by three different computer systems at the Faculty of Science and Earthquake Research Institute, University of Tokyo, and Tohoku University. Therefore, their formats are different. More details are given in individual figure explanations.

The time vs. distance sections of Figs. A1 through A3 are used to constrain the seismic structure of this part of the Pacific Basin (Fig. 5). Further analyses are attempted presently by using more detailed two and three dimensional ray tracing as well as waveform adjustment. A detailed description of the analyses on this matter are given in Part 3 of this issue.

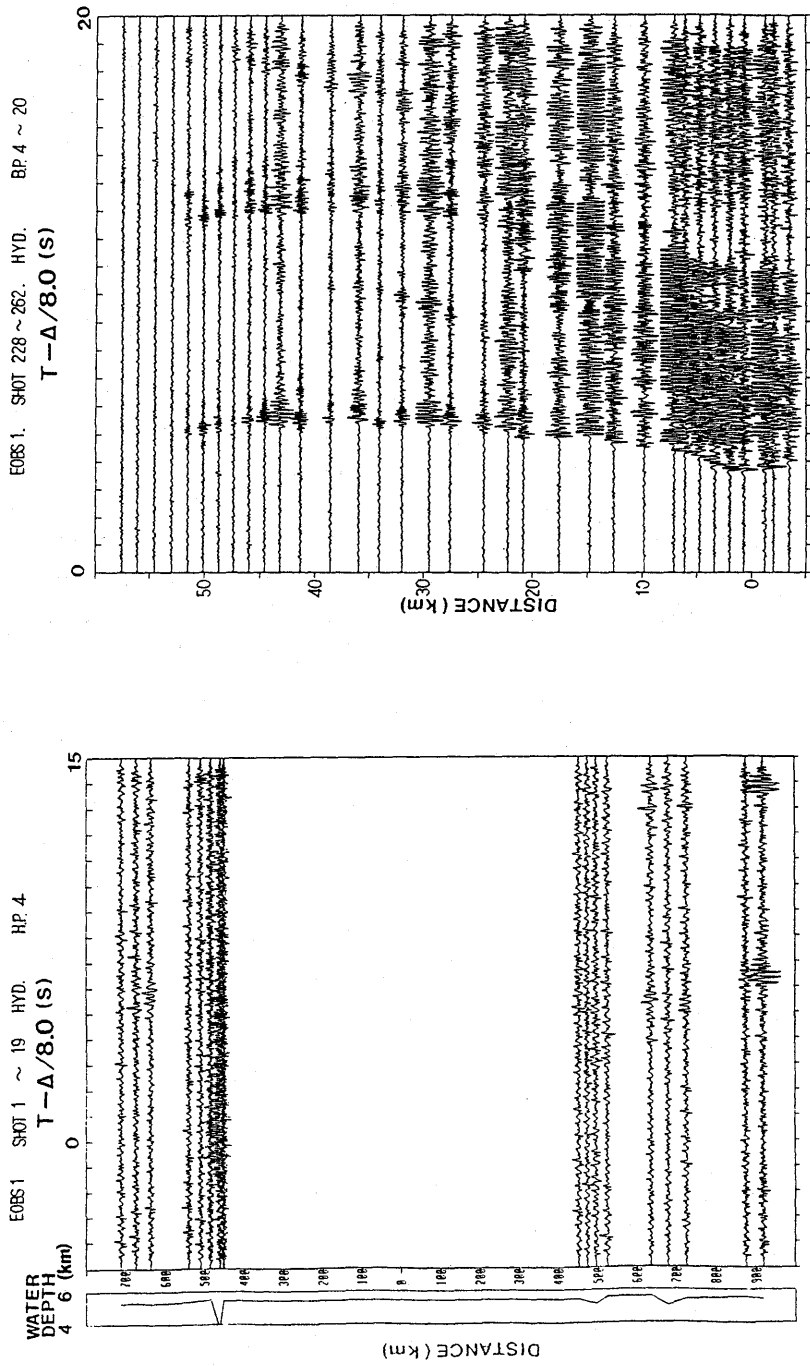


Fig. A1-1. Paste up of time-distance record sections. EOBS1, SHOT 1 through 19 (expressed as SHOT01 and SHOT19 in Table 2). Hydrophone signals, High-pass filtered, cutoff frequency (fcutt) = 4 Hz. Reduction velocity = 8 km/s. No correction to water depth or wave amplitudes applied. Distance on the left, in km. Time on the top, in seconds. Approximate water depths are drawn in the left side frame.

Fig. A1-2. EOBS1, shot No. 228 through 262 (Table 3), Hydrophone signals. Band-pass filtered $f=4-20$ Hz. Others are the same as in Fig. A1-1.

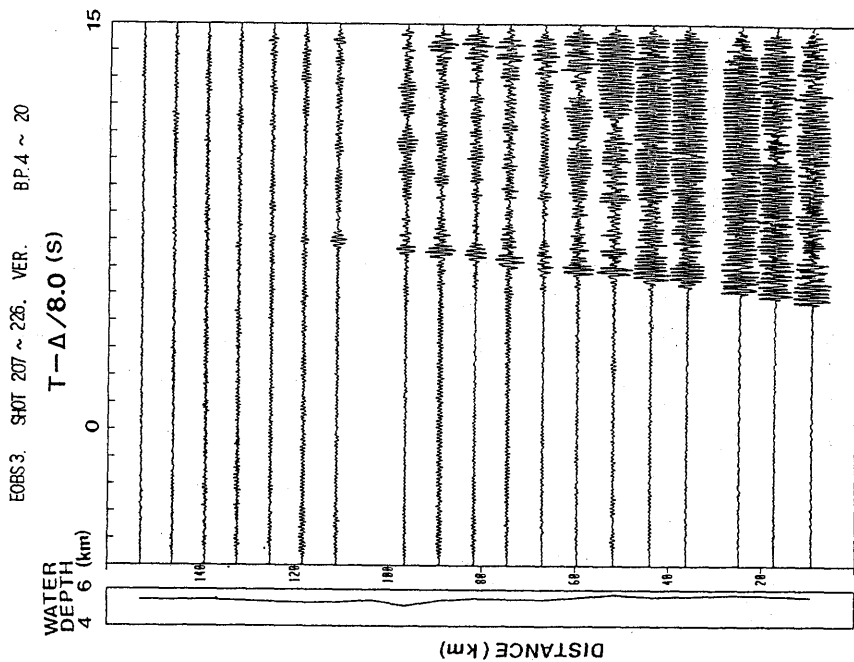


Fig. A1-4. EOBSS, shot No. 207 through 226 (Table 3). Vertical geophone signals. Band-pass filtered $f=4-20$ Hz. Others are the same as in Fig. A1-1.

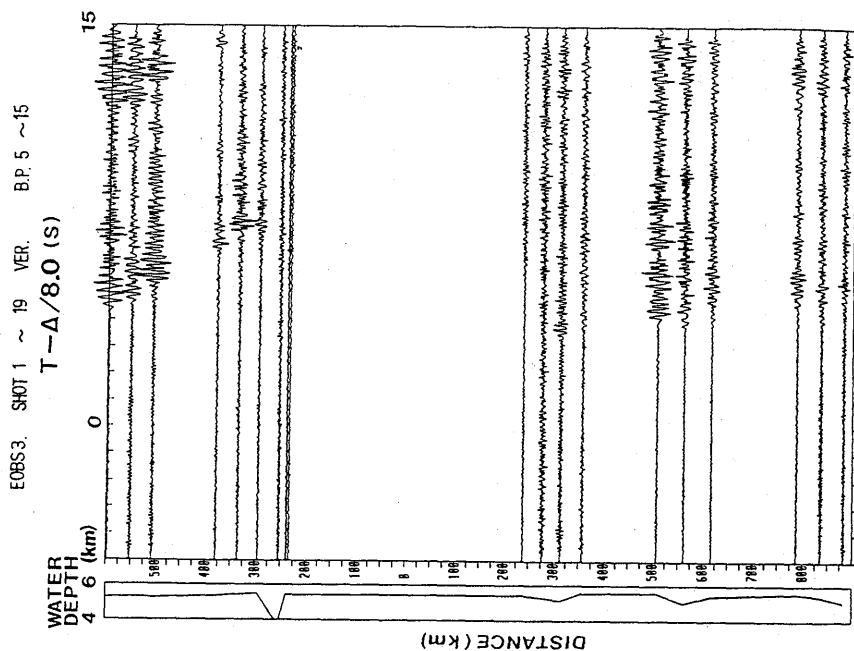


Fig. A1-3. EOBSS, SHOT 1 through 19 (Table 2). Vertical geophone signals. Band-pass filtered $f=5-15$ Hz. Others are the same as in Fig. A1-1.

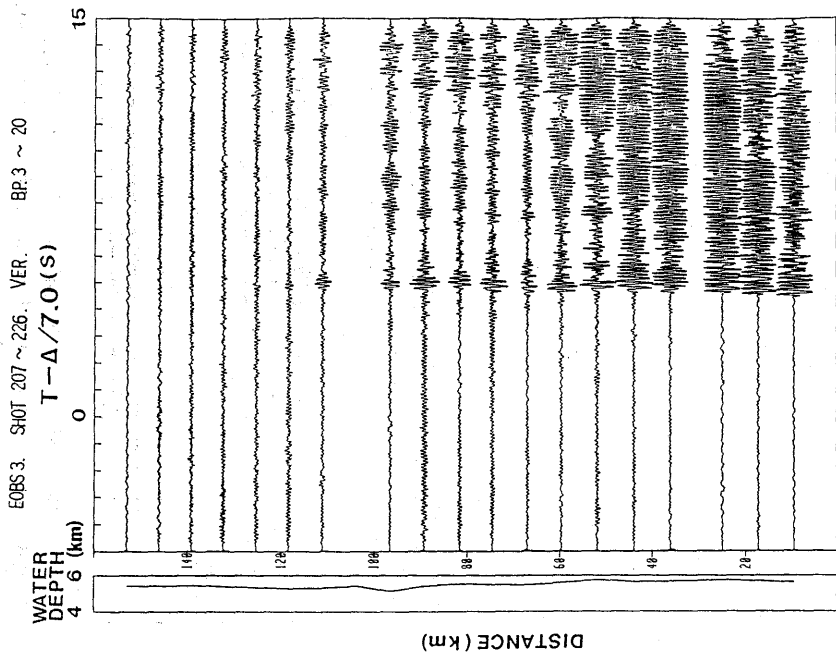
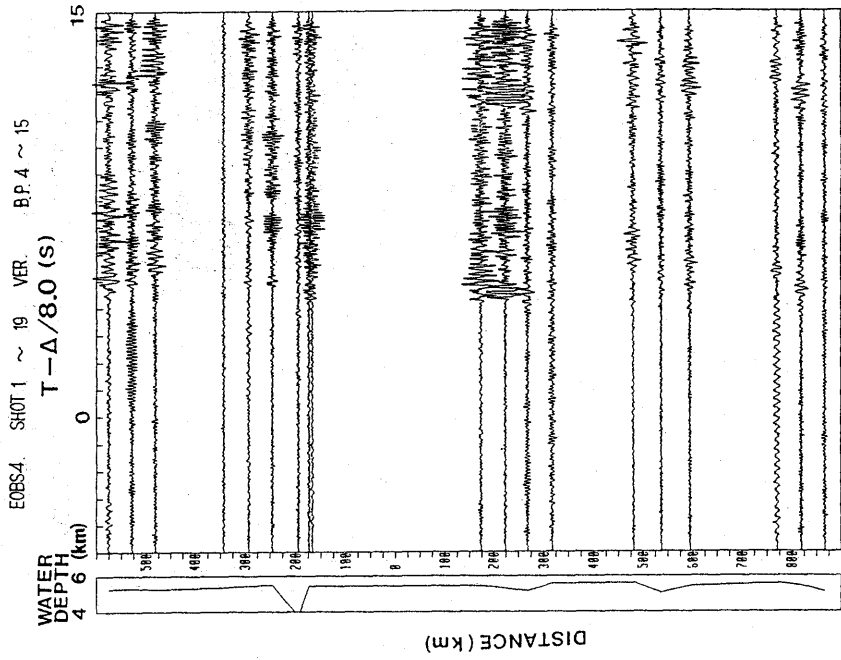


Fig. A1-5. EOBSS3, shot No. 207 through 226. Vertical geophone signals. Band-pass filtered $f=3-20$ Hz. Reduction speed $=7$ km/s. Others are the same as in Fig. A1-1.

Fig. A1-6. EOBSS4, SHOT 1 through 19 (fan shooting: Table 2). Vertical geophone signals. Band-pass filtered $f=4-15$ Hz. Others are the same as in Fig. A1-1.

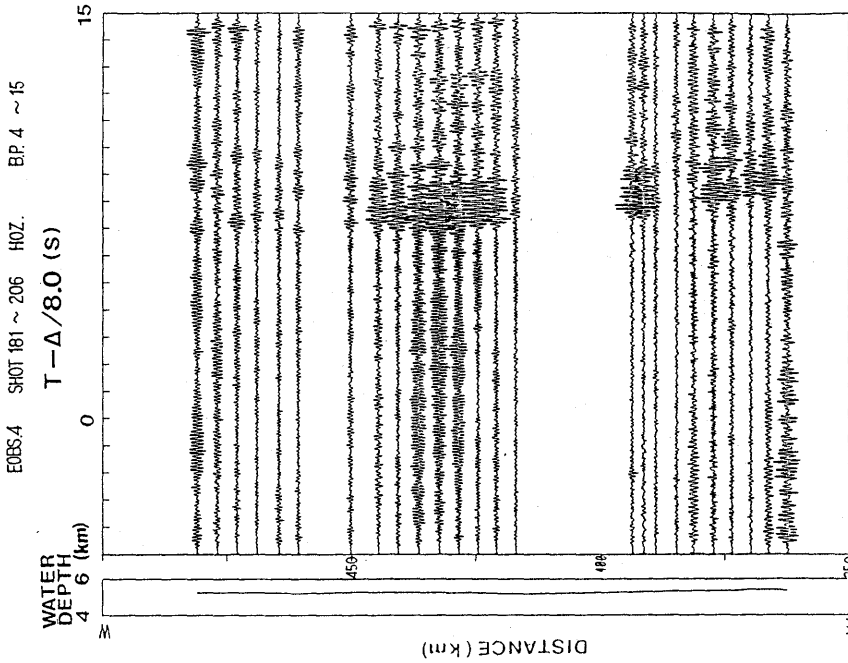


Fig. A1-8. EOBS4, shot No. 181 through 206 (Table 3). Horizontal geophone signals. Band-pass filtered $f=4-15$ Hz. Others are the same as in Fig. A1-1.

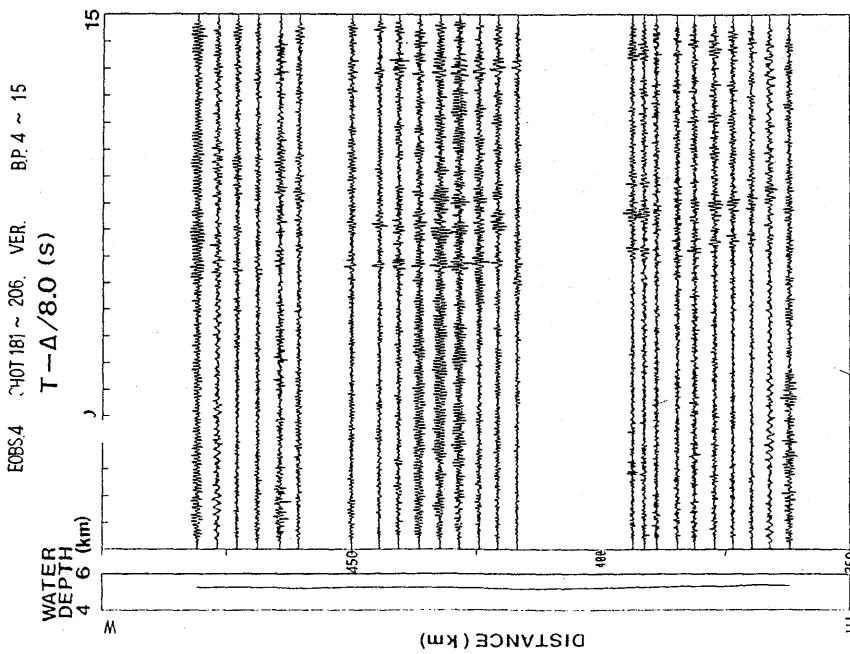


Fig. A1-7. EOBS4, shot No. 181 through 206 (Table 3). Vertical geophone signals. Band-pass filtered $f=4-15$ Hz. Others are the same as in Fig. A1-1.

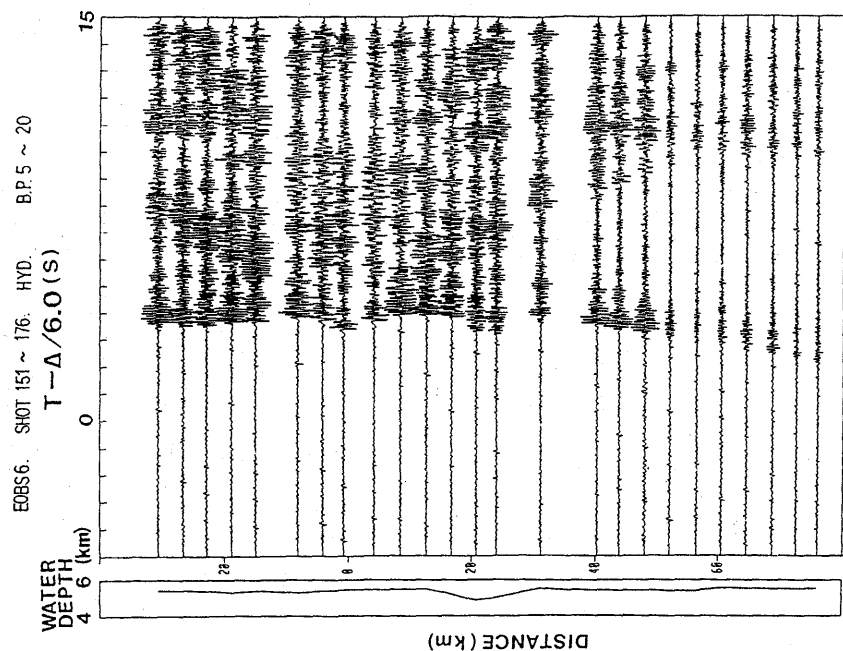


Fig. A1-10. EOBS6, shot No. 151 through 176 (Table 3). Hydrophone signals. Band-pass filtered $f=5-20$ Hz. Reduction speed=6 km/s. Others are the same as in Fig. A1-1.

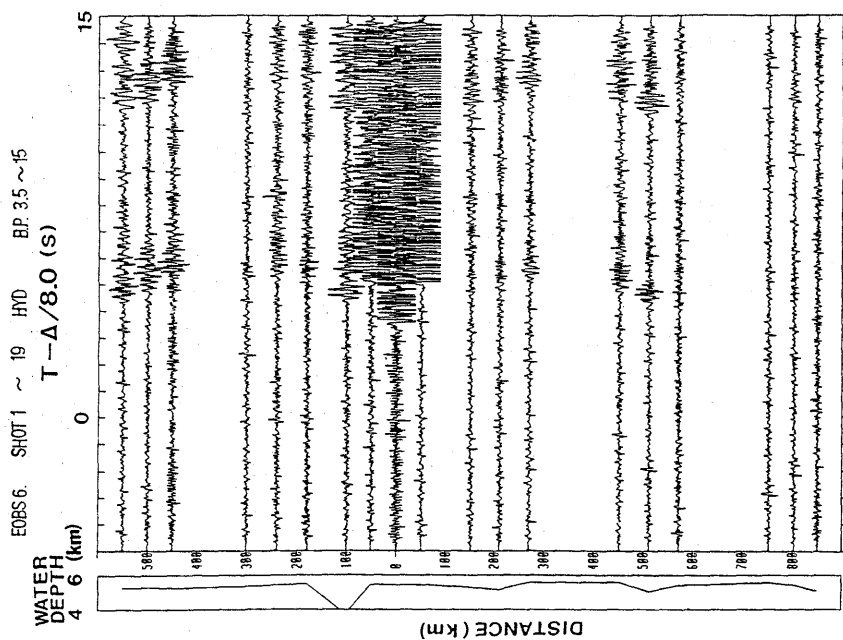


Fig. A1-9. EOBS6, SHOT 1 through 19 (Table 2). Hydrophone signals. Band-pass filtered $f=3.5-19$ Hz. Others are the same as in Fig. A1-1.

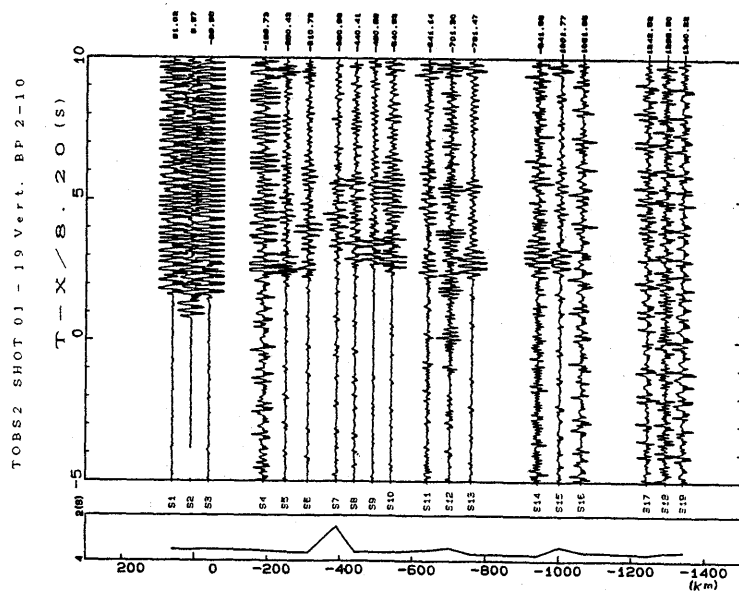


Fig. A2-1. Paste up of time-distance record sections. TOBS2, SHOT 1 through 19 (Table 2; same for all figures of A2). Vertical geophone signals. Band-pass filtered $f=2-10$ Hz. Reduction velocity=8.2 km/s. Correction to water depth and wave amplitudes is applied by normalizing with maximum amplitude of a trace. Distance is shown on the left and right, in km. S denotes shot number. Time on the top, in seconds. Solid curve in the left side frame is approximate bathymetric depth along track line.

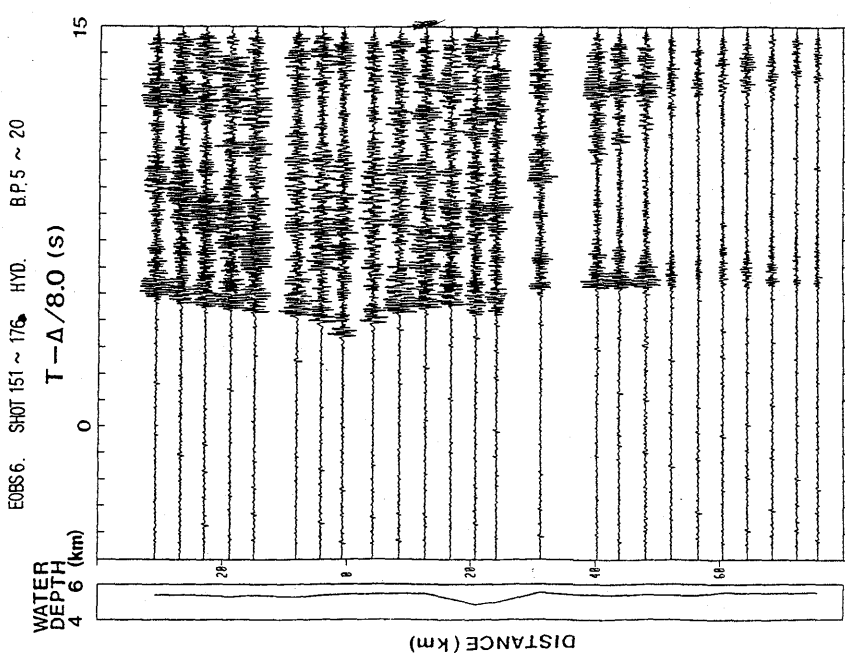


Fig. A1-11. EOBS6, shot No. 151 through 176 (Table 3). Hydrophone signals. Band-pass filtered $f=5-20$ Hz. Others are the same as in Fig. A1-1.

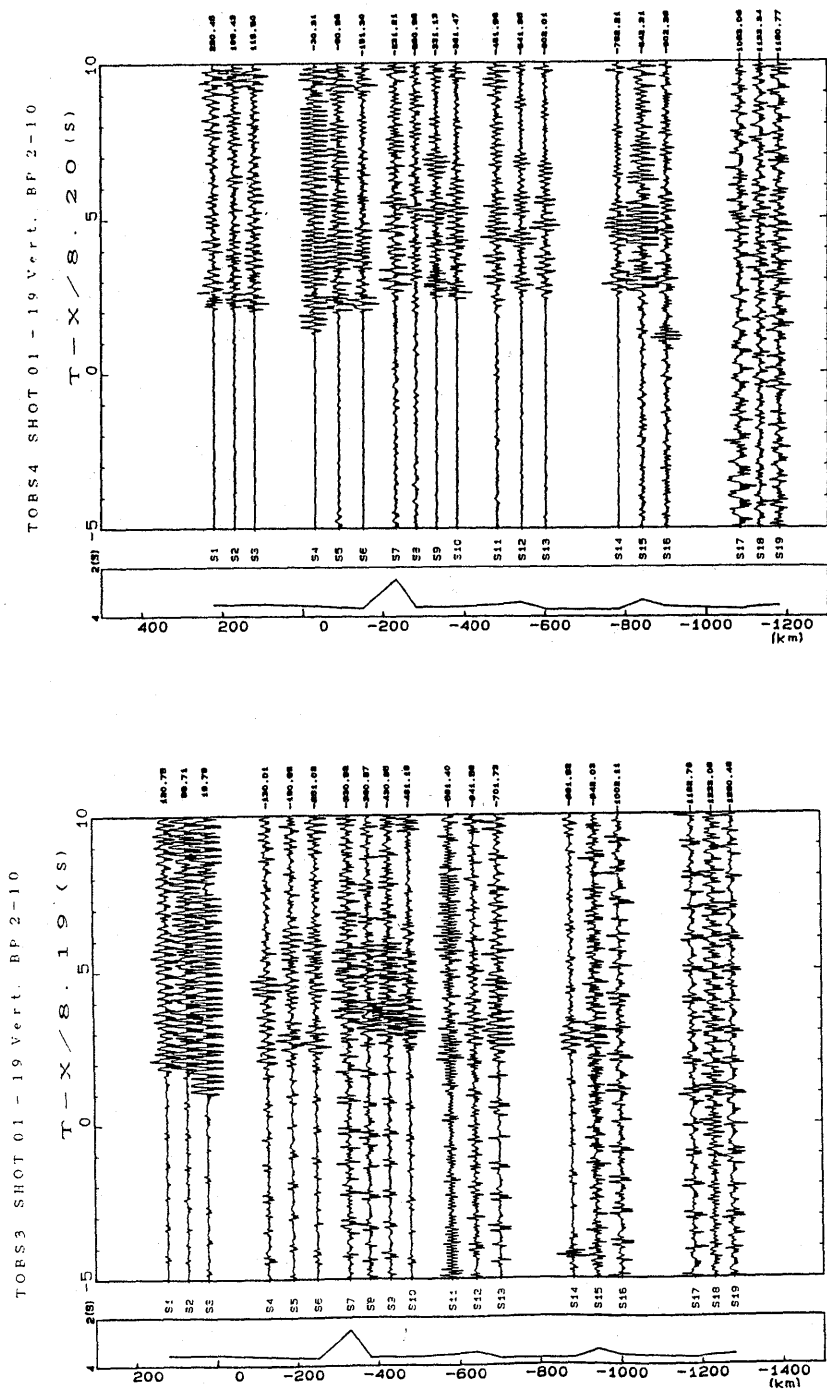


Fig. A2-2. TOBS3, SHOT 1 through 19. Vertical geophone signals. Others are the same as in Fig. A2-1.

Fig. A2-3. TOBS4, SHOT 1 through 19. Vertical geophone signals. Others are the same as in Fig. A2-1.

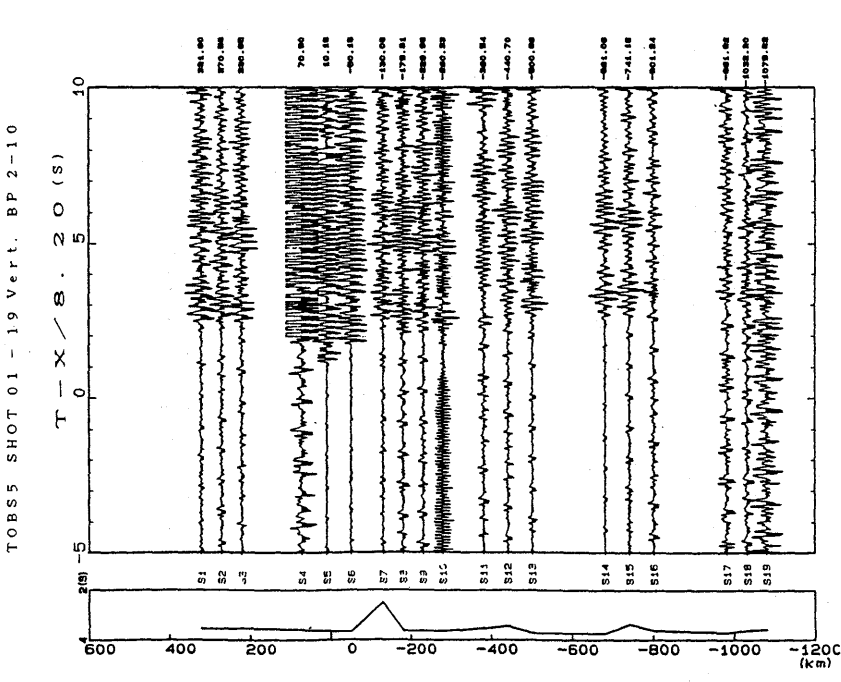
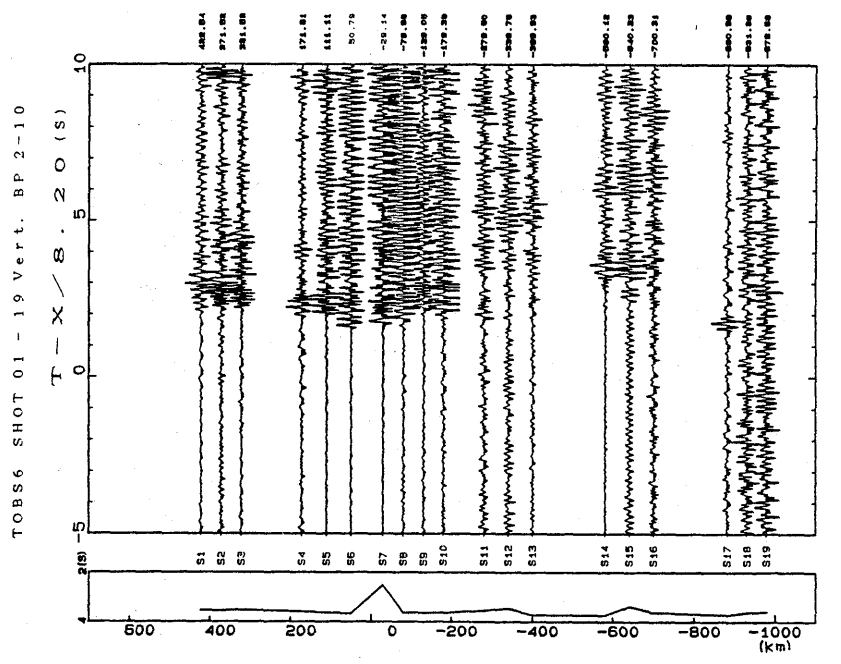


Fig. A2-5. TOBS6, SHOT 1 through 19. Vertical geophone signals. Others are the same as in Fig. A2-1.

Fig. A2-4. TOBS5, SHOT 1 through 19. Vertical geophone signals. Others are the same as in Fig. A2-1.

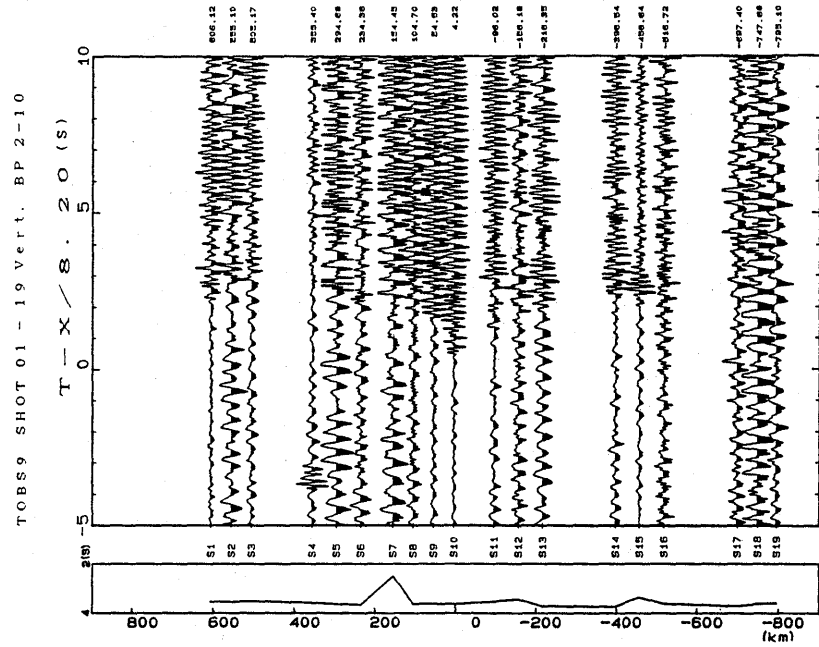


Fig. A2-7. TOBS9, SHOT 1 through 19. Vertical geophone signals. Others are the same as in Fig. A2-1.

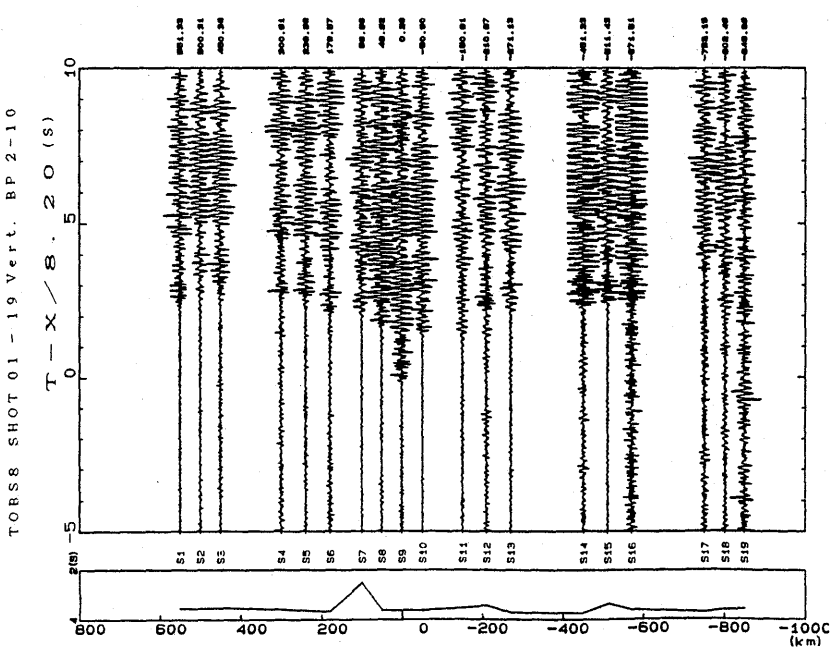


Fig. A2-6. TOBS8, SHOT 1 through 19. Vertical geophone signals. Others are the same as in Fig. A2-1.

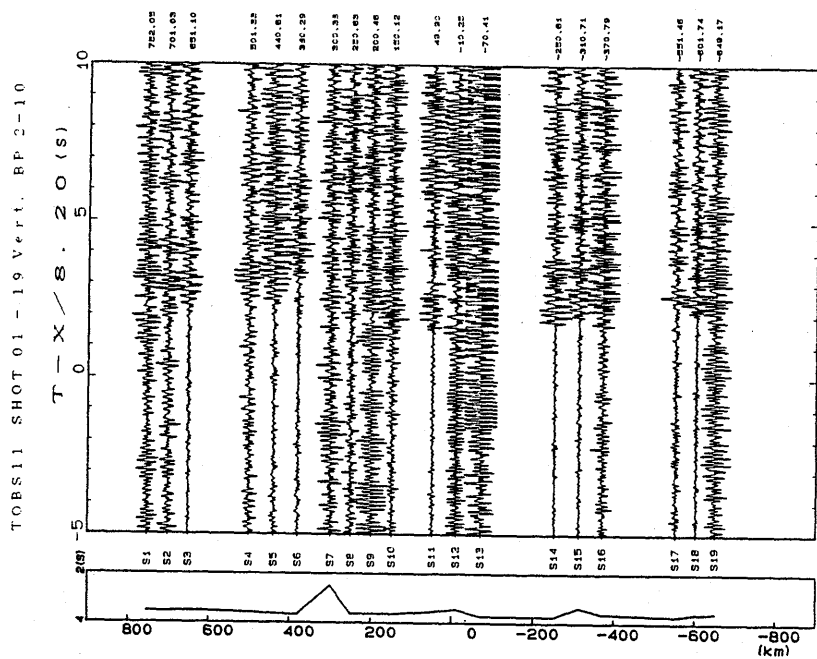


Fig. A2-9. TOBS11, SHOT 1 through 19. Vertical geophone signals. Others are the same as in Fig. A2-1.

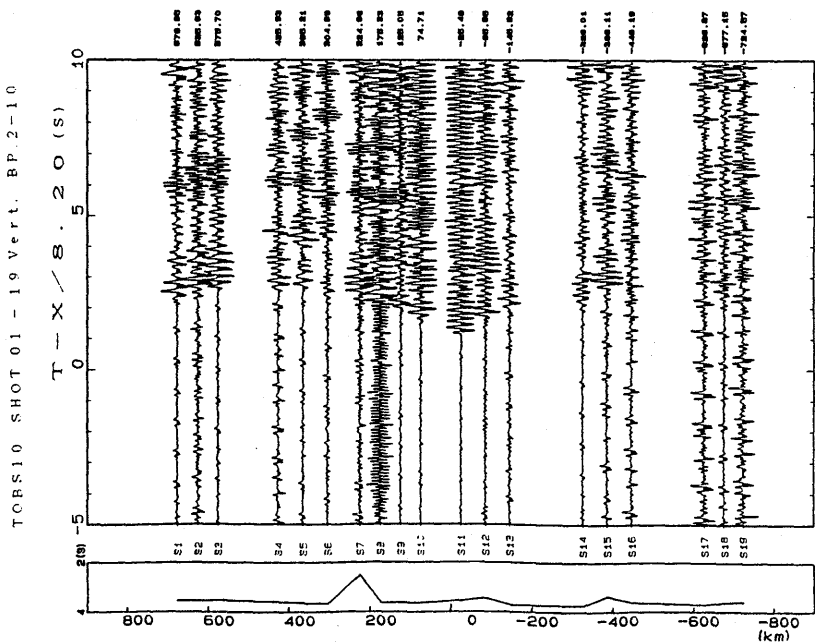


Fig. A2-8. TOBS10, SHOT 1 through 19. Vertical geophone signals. Others are the same as in Fig. A2-1.

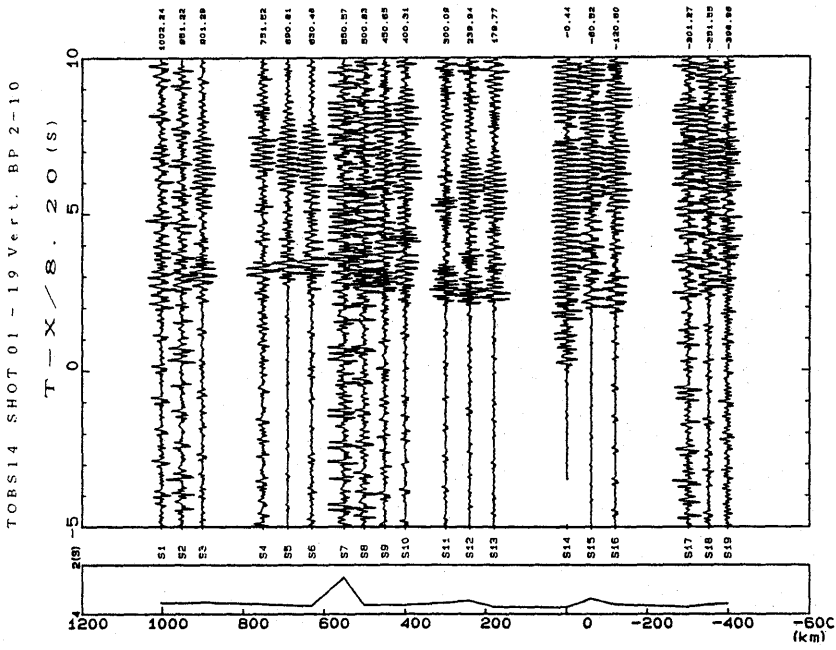


Fig. A2-11. TOBS14, SHOT 1 through 19. Vertical geophone signals. Others are the same as in Fig. A2-1.

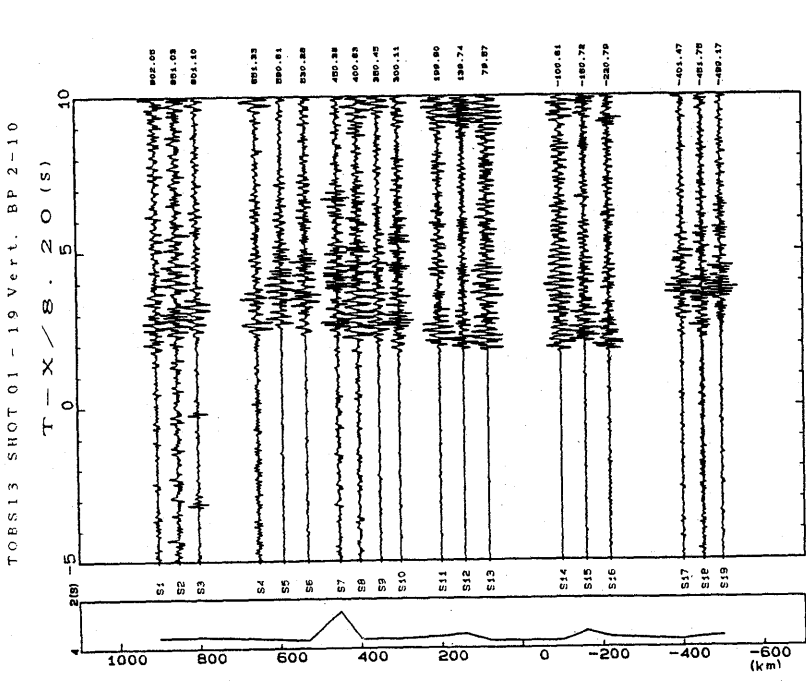


Fig. A2-10. TOBS13, SHOT 1 through 19. Vertical geophone signals. Others are the same as in Fig. A2-1.

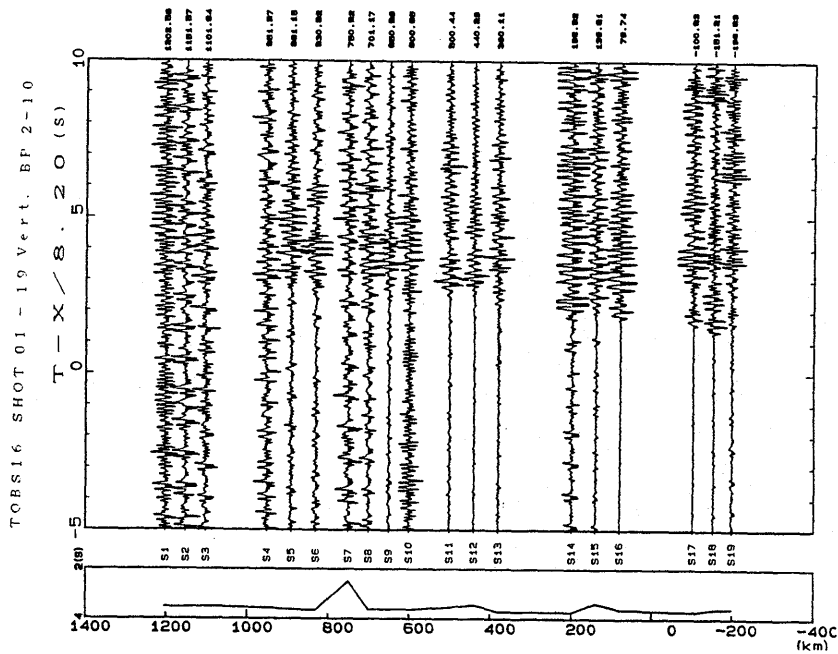


Fig. A2-13. TORS16, SHOT 1 through 19. Vertical geophone signals. Others are the same as in Fig. A2-1.

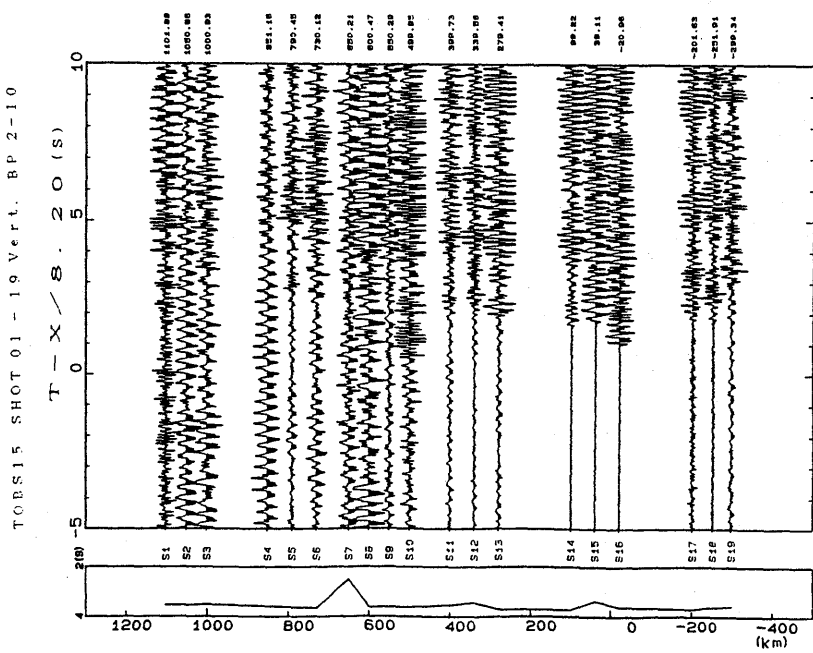


Fig. A2-12. TORS15, SHOT 1 through 19. Vertical geophone signals. Others are the same as in Fig. A2-1.

TOBS20 SHOT 227-285 Vert. BP 5-20

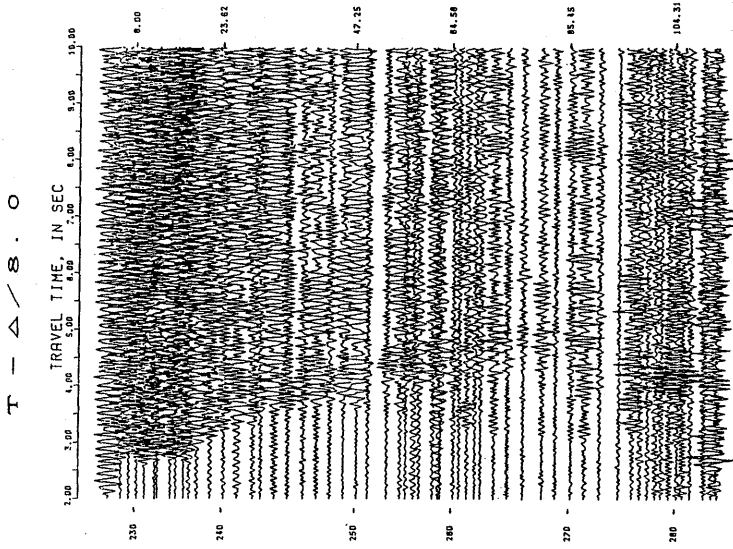


Fig. A3-1. Paste up of time-distance record sections. TOBS20, shot No. 227 through 285 (Table 3). Vertical geophone signals. Band-pass filtered $f=5-20$ Hz. Reduction velocity = 8 km/s. Correction to water depth and wave amplitudes is applied as proportional to square of distance. Distance on the right, in km. Shot numbers on the left. Time on the top, in seconds.

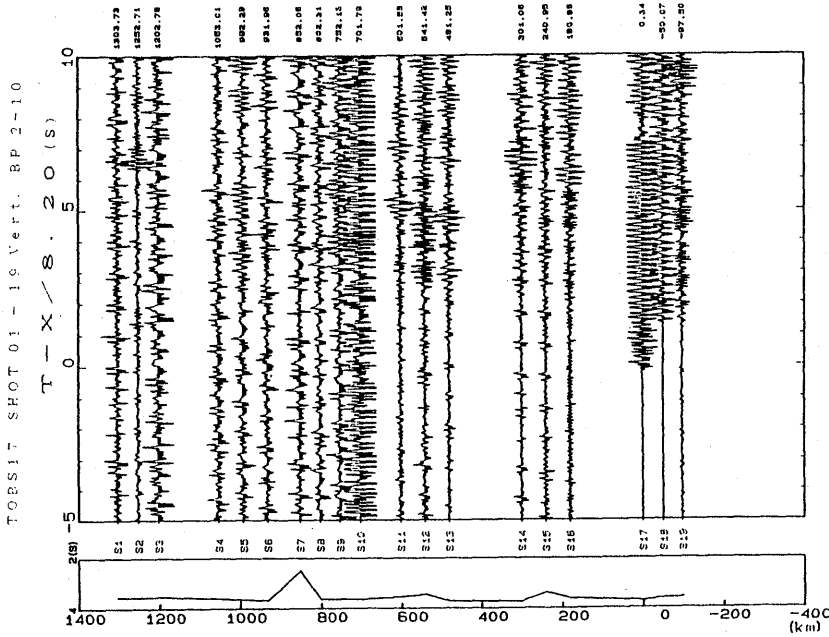
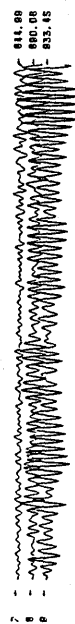
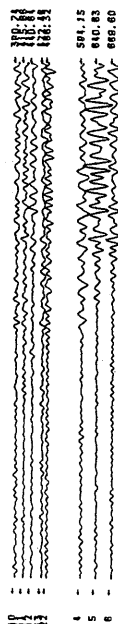
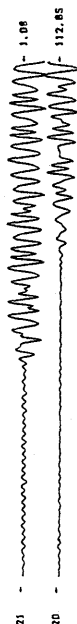
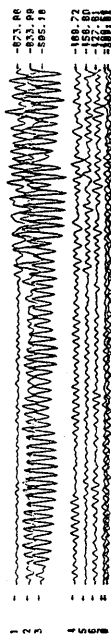
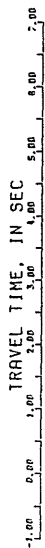


Fig. A2-14. TOBS17, SHOT 1 through 19. Vertical geophone signals. Others are the same as in Fig. A2-1.

TOBS20 SHOT 1-19 Horz. BP 3-12

T - Δ / S . O



TOBS20 SHOT 1-19 Vert. BP 3-12

T - Δ / S . O

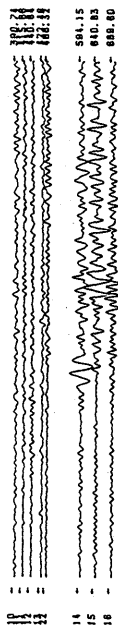
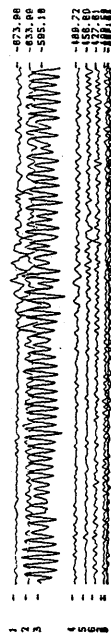
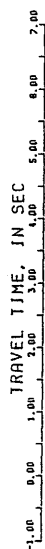


Fig. A3-2. TOBS20, SHOT 1 through 19 (Table 2). Vertical geophone signals. Band-pass filtered, $f=3-12$ Hz. Others are the same as in Fig. A3-1.

Fig. A3-3. TOBS20, SHOT 1 through 19 (Table 2). Horizontal geophone signals. Band-pass filtered, $f=3-12$ Hz. Others are the same as in Fig. A3-1.

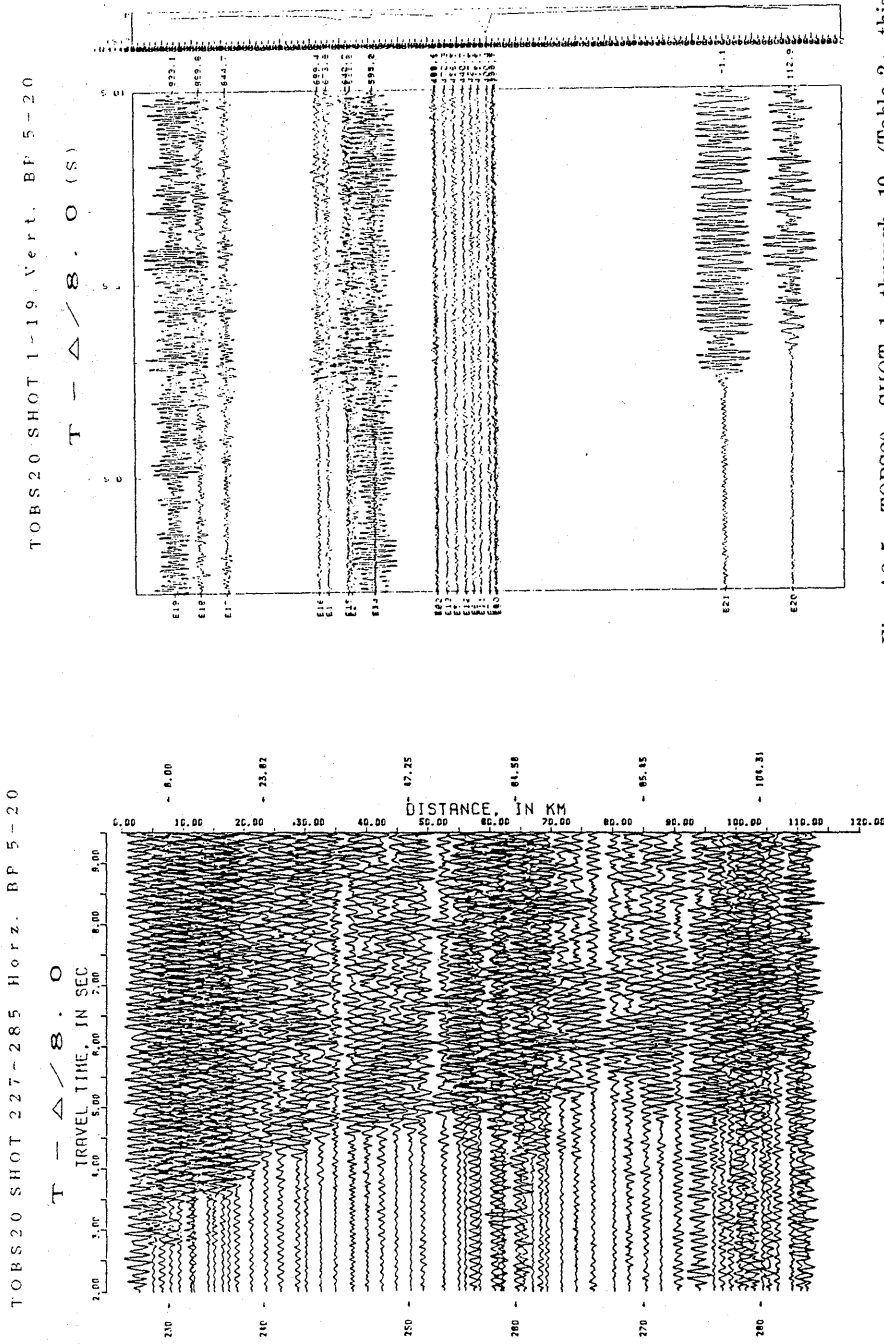


Fig. A3-4. TOBS20, shot No. 227 through 285 (Table 3). Horizontal geophone signals. Band-pass filtered, $f=5-20$ Hz. Others are the same as in Fig. A3-1.

Fig. A3-5. TOBS20, SHOT 1 through 19 (Table 3; this is referred to in all figures after this one). Vertical geophone signals. Band-pass filtered, $f=5-20$ Hz. Others are the same as in Fig. A3-1.

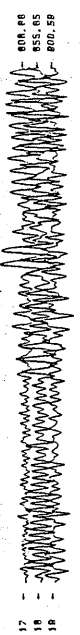
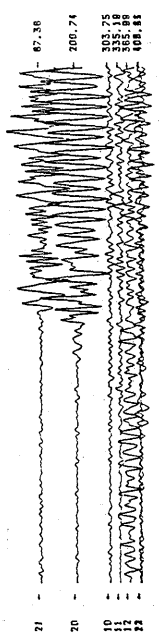
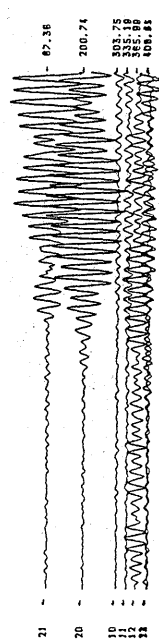
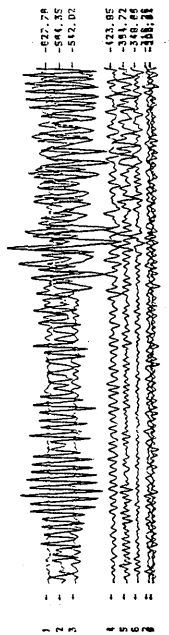
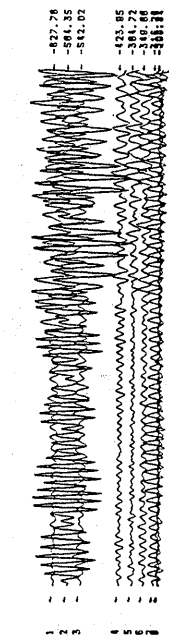
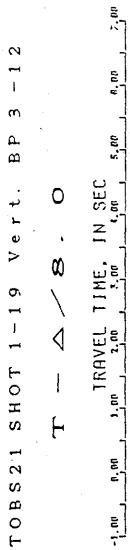
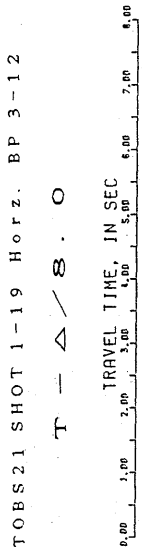


Fig. A3-6. TOBS21, SHOT 1 through 19. Vertical geophone signals. Band-pass filtered, $f=3-12$ Hz. Others are the same as in Fig. A3-1.

Fig. A3-7. TOBS21, SHOT 1 through 19. Horizontal geophone signals. Band-pass filtered, $f=3-12$ Hz. Others are the same as in Fig. A3-1.

TOBS21 SHOT 1-19 Vert. BP 2-8
T - Δ / S . O

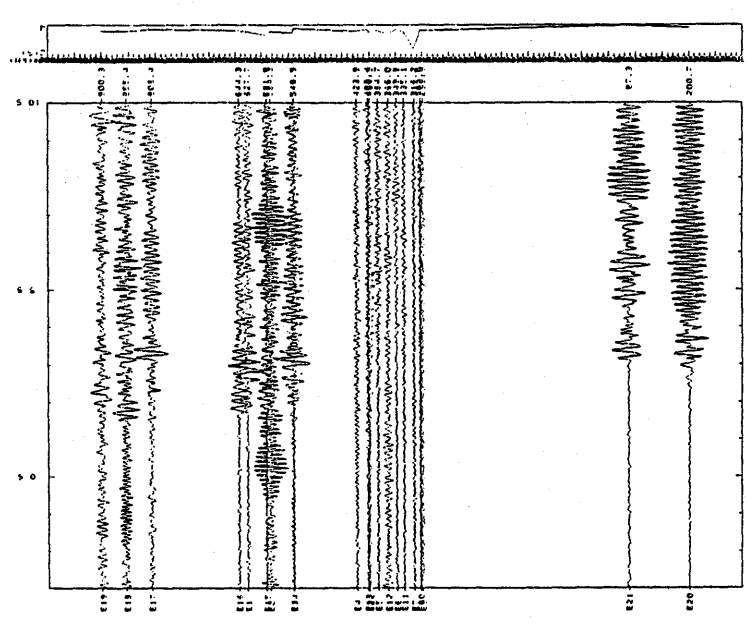


Fig. A3-8. TOBS21, SHOT 1 through 19. Vertical geophone signals. Band-pass filtered, $f=2-8$ Hz. Others are the same as in Fig. A3-1.

TOBS23 SHOT 1-19 Vert. BP 3-12
T - Δ / S . O

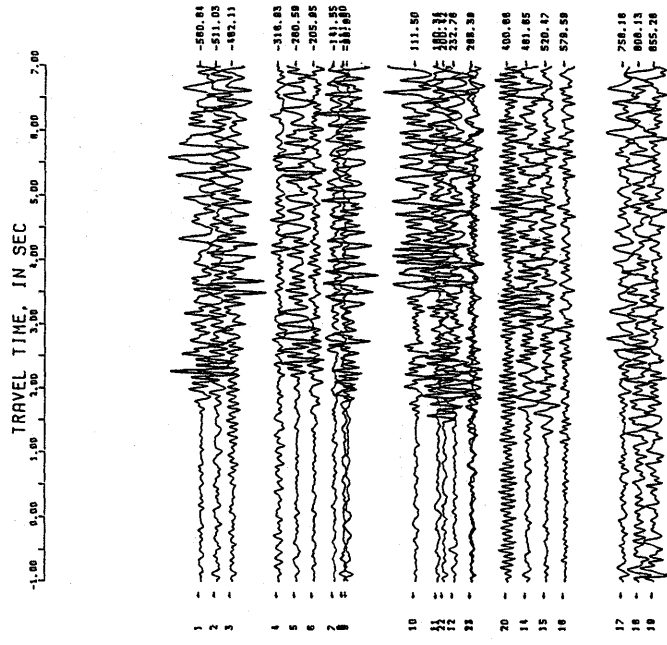
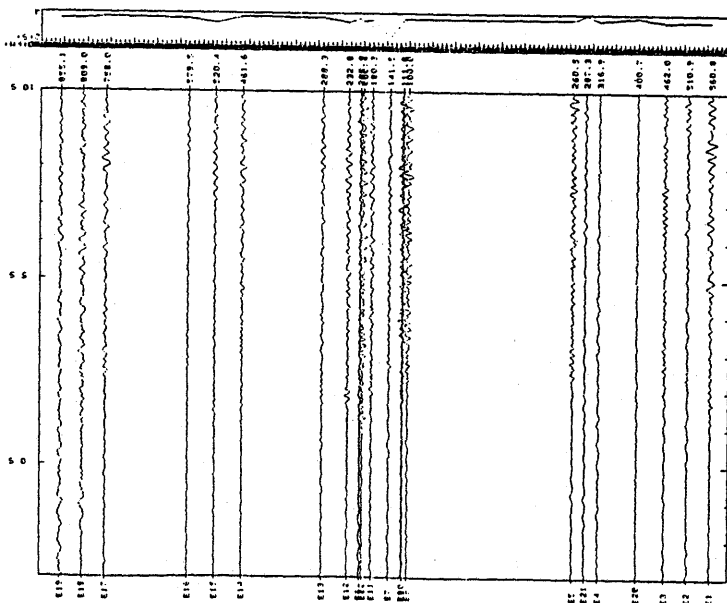


Fig. A3-9. TOBS23, SHOT 1 through 19. Vertical geophone signals. Band-pass filtered, $f=3-12$ Hz. Others are the same as in Fig. A3-1.

TORS23 SHOT 1-19 Vert. BP 2-8

T - Δ / S . O (S)



TOBS23 SHOT 1-19 Horz. BP 3-12

T - Δ / S . O

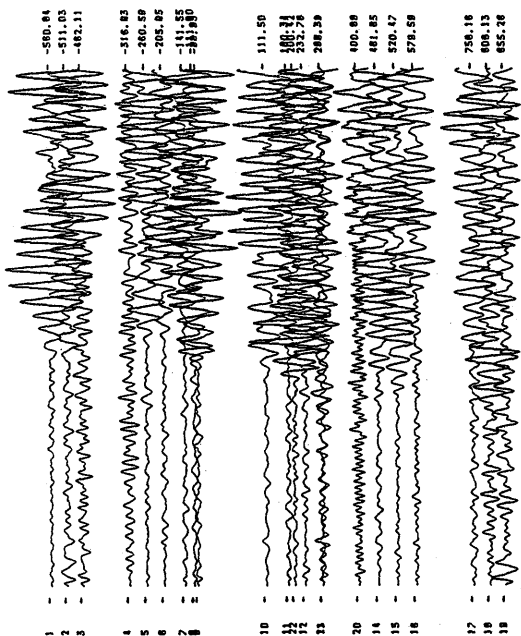
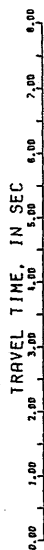
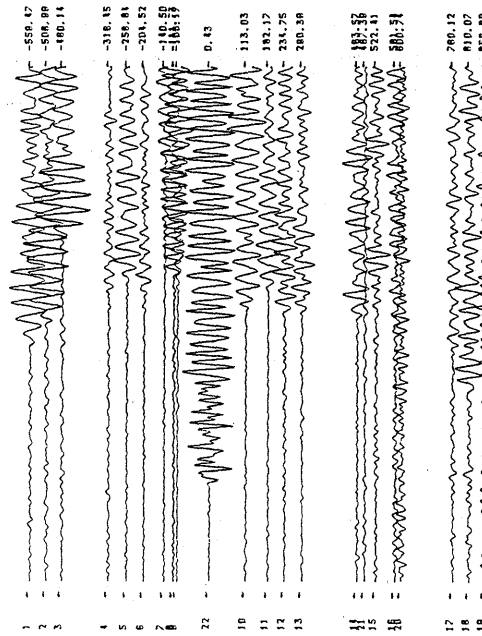
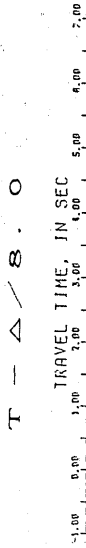


Fig. A3-11. TOBS23, SHOT 1 through 19. Vertical geophone signals. Band-pass filtered, $f=2-8$ Hz. Others are the same as in Fig. A3-1.

Fig. A3-10. TOBS23, SHOT 1 through 19. Horizontal geophone signals. Band-pass filtered, $f=3-12$ Hz. Others are the same as in Fig. A3-1.

TOBS20 SHOT 1-19 Horz. BP 3-12



TOBS24 SHOT 1-19 Vert. BP 3-12

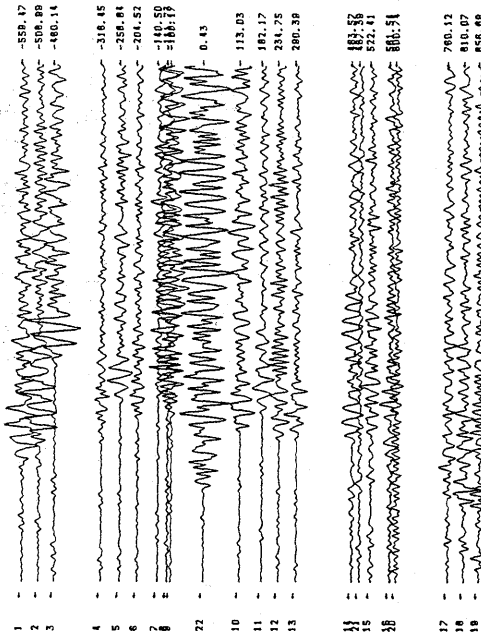
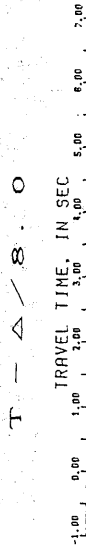


Fig. A3-13. TOBS24, SHOT 1 through 19. Horizontal geophone signals. Band-pass filtered, $f=3-12$ Hz. Others are the same as in Fig. A3-1.

Fig. A3-12. TOBS24, SHOT 1 through 19. Vertical geophone signals. Band-pass filtered, $f=3-12$ Hz. Others are the same as in Fig. A3-1.

TOBS24 SHOT 1-19 Horiz. RP 2-8

T - Δ / S . O (S)

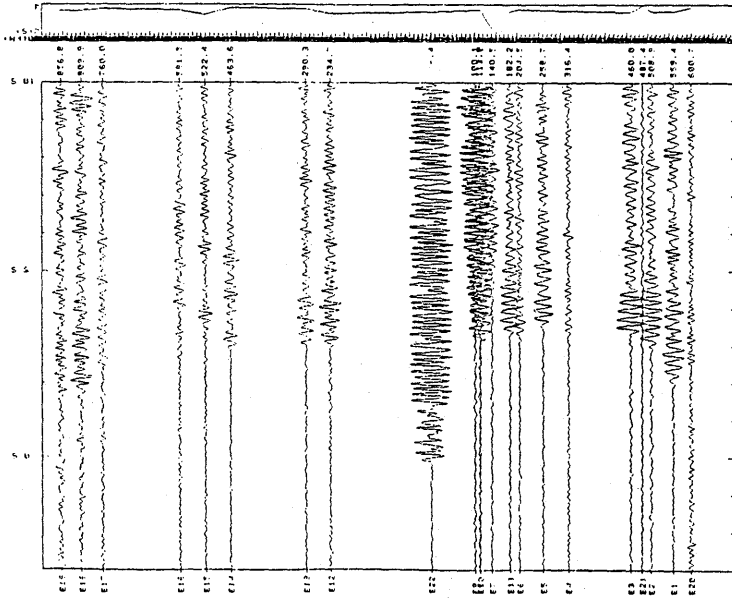


Fig. A3-15. TOBS24, SHOT 1 through 19. Horizontal geophone signals. Band-pass filtered, $f=2-8$ Hz. Others are the same as in Fig. A3-1.

TOBS24 SHOT 1-19 Vert. RP 2-8

T - Δ / S . O (S)

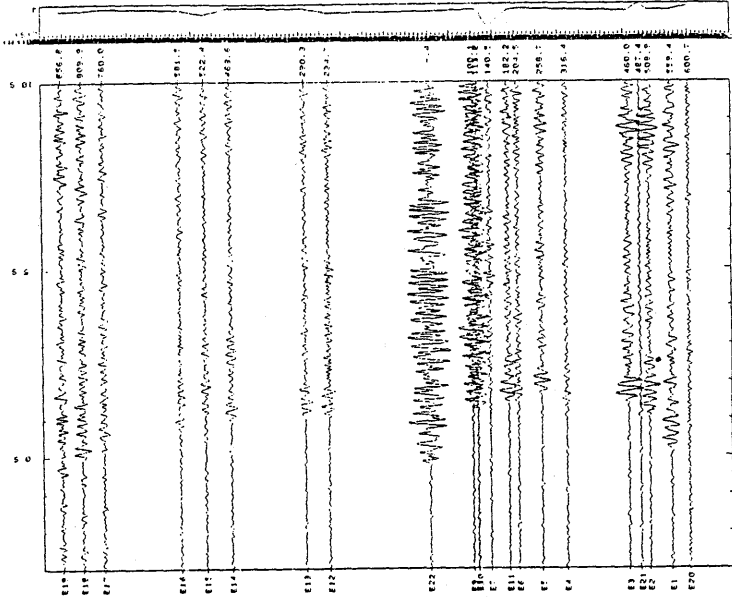


Fig. A3-14. TOBS24, SHOT 1 through 19. Vertical geophone signals. Band-pass filtered, $f=2-8$ Hz. Others are the same as in Fig. A3-1.

DELP 1986年度 北西太平洋研究航海報告

Part 1 計画の概要

DELP 大洋底深部構造研究班

1986年夏季（7月から8月初旬）に DELP 並びに地震予知海底観測両研究グループの協同作業によって、北西太平洋海盆のジャツキー海台と日本北部地域との間の海域に於て地球物理探査航海 (DELP-86) が実施された。本報告の Part 1 から Part 4 にかけて、全長 2100 km に及ぶ十字測線で行われた各種計測・探査につき、DELP-86 航海の成果として報告する。地震音波構造解析の一部は、現在地震予知海底観測研究グループによって継続されている部分もあり、時間的制約から、全てを記述することはできなかった。また各 Part の結果の説明等には、既に他の研究者などによって発表されているものをも引用している。今航海には大学・研究所等 9 機関からの研究者が参加した。本航海の主目的、探査海域、探査期間、探査項目、データ内容及び参加者等に付いて、本文に記載する。航海によって得られた人工地震探査の基礎的データを、今後の解析の便宜に供するために提示した。以上のような点について研究航海の報告を本稿で述べるが、結論・推論については過去の研究などで既に判明していることも含めて議論を行う。なお今回の人工地震観測用大発破音源から東北地方に伝播した人工地震波を利用して、東北日本孤下へ潜り込みつつある太平洋プレートの形状を追認できたことは、他所に既に報告されたが、本稿に合わせ紹介する。その他各分野の細かい研究成果に付いては、Part 2, 3 および 4 に詳しく述べられている。